Published in final edited form as:
Biochem Pharmacol. 2014 June 1; 89(3): 370–385. doi:10.1016/j.bcp.2014.03.017.

Altered Matrix Metalloproteinase-2 and -9 Expression/Activity Links Placental Ischemia and Anti-angiogenic sFlt-1 to Uteroplacental and Vascular Remodeling and Collagen Deposition in Hypertensive Pregnancy

Wei Li, **Karina M. Mata**, **Marc Q. Mazzuca**, and **Raouf A. Khalil**
Vascular Surgery Research Laboratory, Division of Vascular and Endovascular Surgery, Brigham and Women's Hospital and Harvard Medical School, Boston, Massachusetts 02115

Abstract

Preeclampsia is a complication of pregnancy manifested as maternal hypertension and often fetal growth restriction. Placental ischemia could be an initiating event, but the linking mechanisms leading to hypertension and growth restriction are unclear. We have shown an upregulation of matrix metalloproteinases (MMPs) during normal pregnancy (Norm-Preg). To test the role of MMPs in hypertensive-pregnancy (HTN-Preg), maternal and fetal parameters, MMPs expression, activity and distribution, and collagen and elastin content were measured in uterus, placenta and aorta of Norm-Preg rats and in rat model of reduced uteroplacental perfusion pressure (RUPP). Maternal blood pressure was higher, and uterine, placental and aortic weight, and the litter size and pup weight were less in RUPP than Norm-Preg rats. Western blots and gelatin zymography revealed decreases in amount and gelatinase activity of MMP-2 and MMP-9 in uterus, placenta and aorta of RUPP compared with Norm-Preg rats. Immunohistochemistry confirmed reduced MMPs in uterus, placenta and aortic media of RUPP rats. Collagen, but not elastin, was more abundant in uterus, placenta and aorta of RUPP than Norm-Preg rats. The anti-angiogenic factor soluble fms-like tyrosine kinase-1 (sFlt-1) decreased MMPs in uterus, placenta and aorta of Norm-Preg rats, and vascular endothelial growth factor (VEGF) reversed the decreases in MMPs in tissues of RUPP rats. Thus placental ischemia and anti-angiogenic sFlt-1 decrease uterine, placental and vascular MMP-2 and MMP-9, leading to increased uteroplacental and vascular collagen, and growth-restrictive remodeling in HTN-Preg. Angiogenic factors and MMP activators may reverse the decrease in MMPs and enhance growth-permissive remodeling in preeclampsia.

Keywords

myometrium; placenta; blood vessels; Preeclampsia

Correspondence and reprint requests should be addressed to: Raouf A Khalil, MD, PhD Harvard Medical School Brigham and Women's Hospital Division of Vascular Surgery 75 Francis Street Boston, Massachusetts 02115 Tel: (617) 525-8530 Fax: (617) 264-5124 raouf_khalil@hms.harvard.edu.

1. Introduction

Normal pregnancy (Norm-Preg) is associated with significant uteroplacental, hemodynamic and vascular changes. Uterine hypertrophy and distention provide sufficient space for the growing fetus. Placental remodeling and cytotrophoblast invasion of spiral arterioles maintain adequate blood and nutrient supply to the developing fetus. Hemodynamic changes in the maternal circulation such as increased heart rate, plasma volume and cardiac output, and decreased vascular resistance maintain blood supply to different tissues with little change in blood pressure (BP) [1, 2]. These alterations in uteroplacental and maternal circulation involve substantial structural changes and functional adjustments in the uterus, placenta and maternal vasculature [3, 4].

In 5-8% of pregnancies women develop preeclampsia, a condition characterized by hypertension (HTN). If untreated, preeclampsia could lead to eclampsia with severe maternal HTN and seizures [5-7]. Preeclampsia is also often associated with intrauterine growth restriction, accounting for 10-15% of preterm pregnancies [8, 9]. Despite the serious consequences of preeclampsia to the health of mother and fetus, the underlying mechanisms are not fully understood. Placental ischemia could be an initiating event [5, 10], but the linking mechanisms are unclear. Placental ischemia could lead to the release of cytotoxic factors and cause imbalance between anti-angiogenic factors such as soluble fms-like tyrosine kinase-1 (sFlt-1, sVEGFR-1) and soluble endoglin (sEng) and angiogenic factors such as vascular endothelial growth factor (VEGF) and placental growth factor (PlGF) [6, 7, 11-13]. In contrast with the growth-permissive remodelling in Norm-Preg, the extent of uteroplacental and vascular remodelling and the molecular mechanisms via which placental ischemia and anti-angiogenic and angiogenic factors could affect tissue remodelling in HTN-Preg are unclear.

Matrix metalloproteinases (MMPs) are a family of proteases that degrade the extracellular matrix (ECM) and connective tissue proteins [14, 15]. MMPs are produced as pro-MMPs which are cleaved into active MMPs [14, 15]. MMPs include collagenases, gelatinases, stromelysins, matrilysins, and membrane-type MMPs [15]. MMP-2 (gelatinase A) and MMP-9 (gelatinase B) are expressed in bovine uterus [16, 17] and play a role in endometrial tissue remodeling during the estrous cycle, menstrual cycle and pregnancy in animals and human [18-20]. Also, we have previously shown an upregulation of MMP-2 and -9 in the myometrium and aorta of normal pregnant rats, and suggested a role of MMPs in uterine and vascular remodeling [21, 22]. However, the role of MMPs in tissue remodeling, the downstream targets affected, and the upstream mechanisms influencing MMPs activity in HTN-Preg are unclear.

This study was designed to test the hypothesis that alteration of MMPs expression/activity is a major molecular mechanism in the uteroplacental and vascular remodeling associated with placental ischemia and in response to anti-angiogenic factors during HTN-Preg. We used the uterus, placenta and aorta from Norm-Preg rats and a rat model of HTN-Preg produced by reduction in uteroplacental perfusion pressure (RUPP) to investigate whether: 1) Alterations in uteroplacental and vascular tissue remodeling are related to changes in MMP-2 and -9 expression/activity in RUPP compared with Norm-Preg rats, 2) The changes in

uteroplacental and vascular tissue remodeling and MMP activity reflect changes in the downstream target protein collagen or elastin, and 3) Anti-angiogenic and angiogenic factors are upstream modulators of MMPs expression/activity in Norm-Preg and RUPP rats.

2. Methods

2.1. Animals

Time-pregnant (day 11 of gestation) Sprague-Dawley rats (12 week of age) from Charles River Laboratories (Wilmington, MA, USA) were maintained in the animal facility on *ad libitum* standard rat chow and tap water in 12-hr light-dark cycle. On day 13 of pregnancy, pregnant rats allocated to the RUPP group were anesthetized by inhalation of isoflurane, the abdominal cavity was opened, the lower abdominal aorta was exposed, and a silver clip (0.203 mm ID) was placed around the aorta above the iliac bifurcation as previously described [23-26]. This procedure reduces uterine perfusion pressure in the gravid rat by ~40% [27]. Since compensation of blood flow to the placenta occurs through an adaptive increase in ovarian blood flow, a silver clip (0.1 mm ID) was also placed on the main uterine branches of both the right and left ovarian arteries. Norm-Preg rats were sham operated. RUPP rats in which the clipping procedure resulted in maternal death or total reabsorption of the fetuses were excluded from the data analyses. All procedures were performed in accordance with the National Institutes of Health Guide for the Care of Laboratory Animal Welfare Act, and the guidelines of the Animal Care and Use Committee at Harvard Medical School.

2.2. Body weight and blood pressure

On day 19 of gestation, after measuring body weight, BP was measured via a PE-50 carotid arterial catheter connected to a pressure transducer.

2.3. Tissue preparation

After measuring BP, rats were euthanized by inhalation of CO_2, the abdominal and thoracic cavities were opened, and the uterus, thoracic aorta, heart and kidneys were excised and placed in Krebs solution. The pregnant uterus was cut open, the placentae and pups were separated, gently blotted between filter papers, and the litter size and individual pup and placenta wet weight were recorded. The uterus, placenta, thoracic aorta (from the heart to the diaphragm), heart and kidneys were cleaned of adipose tissue, gently blotted and their wet weight was also recorded. The uterus, placenta and aorta were then cut into 5 mm wide segments, and experiments were performed on 8 to 12 tissue segments from each rat, 4 to 9 rats per group. Some uterine, placental and aortic segments from Norm-Preg rats were incubated in the presence of sFlt-1 (0.1 μg/ml, R&D Systems, Minneapolis, MN) with or without VEGF (0.1 μg/ml, R&D Systems) for 48 hr in tissue culture medium. Also, some uterine, placental and aortic segments from RUPP rats were incubated with VEGF (0.1 μg/ml) for 48 hr in tissue culture medium. The culture medium was changed and fresh sFlt-1 and/or VEGF was added every 24 hr.

2.4. Western blots

Uterine, placental and aortic strips were homogenized in a homogenization buffer containing 20 mM 3-[N-morpholino] propane sulfonic acid, 4% SDS, 10% glycerol, 2.3 mg dithiothreitol, 1.2 mM EDTA, 0.02% BSA, 5.5 μM leupeptin, 5.5 μM pepstatin, 2.15 μM aprotinin and 20 μM 4-(2-aminoethyl)-benzenesulfonyl fluoride, using a 2-ml tight-fitting homogenizer (Kontes Glass Co., Vineland, NJ). The homogenate was centrifuged at 10,000 g for 10 min, the supernatant was collected, and protein concentration was determined using a protein assay kit (Bio-Rad, Hercules, CA). Protein extracts (20 μg) were combined with an equal volume of 2X Laemmli loading buffer, boiled for 5 min, and size fractionated by electrophoresis on 8% SDS-polyacrylamide gels. Proteins were transferred from the gel to a nitrocellulose membrane by electroblotting. Membranes were incubated in 5% nonfat dry milk in TBS-Tween for 1 hr and then overnight at 4°C with polyclonal rabbit anti-MMP-2 (sc-10736, 1:1000), or anti-MMP-9 antibody (sc-10737, 1:1000) (Santa Cruz Biotechnology, Dallas, TX). Membranes were washed 3 times for 15 min each in TBS-Tween then incubated with horseradish peroxidase-conjugated secondary antibody (1:1000) for 2 hr, and the immunoreactive bands were detected using enhanced chemiluminescence (ECL) Western blotting detection reagent (GE Healthcare Bio-Sciences, Piscataway, NJ). The blots were subsequently reprobed for β-actin (1:5000). Data were analyzed by optical densitometry and ImageJ software (National Institutes of Health, Bethesda, MD). The densitometry values represented the pixel intensity normalized to β-actin to correct for loading as previously described [21, 22].

2.5. Gelatin zymography

Uterine, placental and aortic tissue homogenate (without dithiothreitol) was subjected to electrophoresis on 8% SDS polyacrylamide gel containing 0.1% gelatin (Sigma, St. Louis, MO). The gel was then incubated in a zymogram renaturing buffer containing 2.5% Triton X-100 (Sigma) with gentle agitation for 30 min at room temperature. The gel was then equilibrated in a zymogram developing buffer (pH 6.7) containing 50 mM Tris-base, 0.2 M NaCl, 5 mM $CaCl_2$, 0.02% Brij35 (Fisher Scientific, Pittsburgh, PA), and 1 μM $ZnCl_2$ (Sigma) for 30 min at room temperature, then incubated in the zymogram developing buffer at 37°C for 16 hr. The gel was stained with 0.5% coomassie blue R-250 (Sigma) for 30 min, then destained with an appropriate coomassie R-250 destaining solution (methanol : acetic acid : water = 50 : 10 : 40). Areas corresponding to MMP-2 and MMP-9 activity appeared as clear bands against a dark blue background. The clear bands were analyzed by optical densitometry and ImageJ software, and the integrated protease activity density was measured as pixel intensity × mm^2 normalized to actin intensity as previously described [21, 22].

2.6. Histology and quantitative morphometry

To assess if HTN-Preg is associated with adaptive uterine, placental or vascular tissue changes in total wall thickness or the relative thickness of the blood vessel intima, media and adventitia, tissues from Norm-Preg and RUPP rats were cryopreserved in Tissue-Tek 4583 optimal cutting temperature compound (OCT, Fisher Scientific) and stored at −20°C. Cross-sectional 6 μm thick cryosections from the middle segment of the uterus, placenta and

aorta were placed on glass slides and prepared for staining with hematoxylin and eosin. Stained sections were coded and labeled in a blinded fashion. Images were acquired on a Nikon microscope using the same microscope magnification, light intensity and camera gain and analyzed using ImageJ software. Outlines of the tissue lumen and external wall were defined, and the total wall thickness and the relative thickness of the vascular intima, media and adventitia were measured as previously described [22, 28].

2.7. Collagen and elastin staining

Uterine, placental and aortic cryosections were stained with Picro-Sirius Red for collagen and Modified Verhoff's-Van Gieson for elastin [29, 30]. Images were acquired on a Nikon microscope using the same microscope magnification, light intensity and camera gain and analyzed using ImageJ. Outlines of the tissue lumen and external wall were defined and the red (collagen) or black (elastin) staining as % of total wall area was measured

2.8. Immunohistochemistry

To determine the tissue distribution of MMP-2 and -9, cryosections of the uterus, placenta and aorta were thawed and fixed in ice-cold acetone for 30 min. Endogenous peroxidase was quenched in 1.5% H_2O_2 solution for 30 min, and nonspecific binding was blocked in 10% horse serum for 30 min. Tissue sections were incubated with polyclonal MMP-2 (1:100) or MMP-9 (1:100) antibody. After rinsing with PBS, tissue sections were incubated with biotinylated anti-rabbit secondary antibody, rinsed with PBS, then incubated with avidin-labeled peroxidase (VectaStain Elite ABC Kit, Vector Laboratories, Burlingame, CA). Positive labeling was visualized using diaminobenzadine and appeared as brown spots. Negative control slides were run simultaneously with no primary antibody. Specimens were counterstained with hematoxylin for 40 sec, rinsed with PBS, topped with cytoseal 60, and covered with slide coverslips. Images were acquired on a Nikon microscope using the same microscope magnification, light intensity and camera gain, and analyzed using ImageJ software. The total number of pixels in the tissue section image was defined, then the number of brown spots (pixels) was counted and presented as % of total pixels. The number of pixels in the specific vascular layer (intima, media and adventitia) was also defined and transformed into the area in μM^2 using a calibration bar. The number of brown spots (pixels) representing MMP-2 and MMP-9 in each vascular layer was then counted and presented as number of pixels/μM^2 [28].

2.9. Solutions and drugs

Krebs' solution was used for tissue dissection and contained (in mM): 120 NaCl, 5.9 KCl, 25 $NaHCO_3$, 1.2 NaH_2PO_4, 11.5 dextrose, 2.5 $CaCl_2$, 1.2 $MgCl_2$, at pH 7.4, and bubbled with 95% O_2 5% CO_2. The tissue culture medium used to pretreat the tissues with anti-angiogenic or angiogenic factors was composed of Minimum Essential Medium supplemented with penicillin, streptomycin, and amphotericin B (Invitrogen, Grand Island, NY). Phosphate buffered saline (PBS) was used to rinse the slides in the immunohistochemistry experiments and contained (in mM): 137 NaCl, 2.7 KCl, 8 Na_2HPO_4, 2 KH_2PO_4, at pH 7.4. Stock solutions of sFlt-1 and VEGF (R&D Systems) were prepared in distilled H_2O. All other chemicals were of reagent grade or better.

2.10.Statistical analysis

Experiments were conducted on uterus, placenta and aorta isolated from 4 to 9 different rats per group (Norm-Preg vs. RUPP rats) and cumulative data were presented as means±SEM, with the “n” value representing the number of rats per group. Data were analyzed and plotted using Prism (v.5.01; GraphPad software, San Diego, CA). Data were first analyzed using one way ANOVA. When a statistical difference was observed, data were further analyzed using Bonferroni's *post hoc* correction for multiple comparisons. Student's unpaired *t*-test was used for comparison of two means. Differences were statistically significant when $P < 0.05$.

3. Results

Maternal measurements on day 19 of pregnancy showed that BP was higher in RUPP than Norm-Preg rats (**Fig. 1A**). The body weight of intact animals was significantly reduced in RUPP compared with Norm-Preg rats (**Fig. 1B**). However, after animal sacrifice and removing the uterus, placentae and pups, the body weight was not significantly different between RUPP and Norm-Preg rats (**Fig. 1B**). Further analysis of the data indicated that the maternal body weight without uterus vs. with uterus was significantly reduced in Norm-Preg rats ($P<0.01$), but not significantly different in RUPP rats ($P=0.21$) (**Fig. 1B**). Also, the maternal body weight without uterus as percentage of body weight with uterus was significantly reduced ($P<0.01$) in Norm-Preg (88.5±0.5%) compared with RUPP rats (94.4±0.4%), further suggesting that the decreased body weight in RUPP vs. Norm-Preg rats is related to differences in the weight of the uterus, placentae and pups. In effect, the uterus weight (without placentae or pups), the average individual placenta weight and thoracic aorta weight were less in RUPP than Norm-Preg rats (**Fig. 1C**). In contrast, the heart and average kidney weight was not different between RUPP and Norm-Preg rats (**Fig. 1C**). Fetal measurements also showed that both litter size (number of pups) (**Fig. 1D**) and individual fetal weight (**Fig. 1E**) were reduced in RUPP compared with Norm-Preg rats. The decreased individual pup weight in RUPP rats is unlikely because the dams are smaller, as the maternal body weight without uterus was not significantly different in RUPP vs. Norm-Preg rats (Fig. 1B).

We then measured the protein amount of uterine, placental and vascular MMPs in Norm-Preg and RUPP rats. Western blots revealed immunoreactive bands corresponding to pro-MMP-2 (72 kDa), MMP-2 (63 kDa), pro-MMP-9 (92 kDa) and MMP-9 (82 kDa) in uterus, placenta and aorta of Norm-Preg rats (**Fig. 2**). The amount of pro-MMP-2, MMP-2, pro-MMP-9 and MMP-9 was significantly reduced in uterus (**Fig. 2A**), placenta (**Fig. 2B**) and aorta (**Fig. 2C**) of RUPP compared with Norm-Preg rats. Further analysis of the Western blot data showed that the amount of MMP-2 was greater than the pro-MMP-2 form in the uterus, placenta and aorta of both Norm-Preg and RUPP rats, and the MMP-2/pro-MMP-2 ratio in all tissues tested was not significantly different in RUPP vs. Norm-Preg rats (**Fig. 2**). While the amount of MMP-9 was less than the pro-MMP-9 form in the uterus, placenta and aorta of both Norm-Preg and RUPP rats, the MMP-9/pro-MMP-9 ratio in the three tissues was not significantly different in RUPP vs. Norm-Preg rats (**Fig. 2**).

Gelatin zymography analysis using uterine, placenta and aortic tissue homogenate from Norm-Preg rats revealed proteolytic bands corresponding to pro-MMP-2, MMP-2, pro-MMP-9, and MMP-9 (**Fig. 3A, 3C, 3E**), and the cumulative intensities of the bands were analyzed and presented in accompanying graphs (**Fig. 3**). The intensity of the bands was dependent on the amount of loaded protein and showed concentration-dependent increases from 0.1, 0.2 to 0.5 μg protein, and clearly discernible bands at 1 and 2 μg protein. Further increases in loaded protein to 5 and 10 μg showed insignificant increases in proteolytic activity, and the MMP bands appeared almost saturated (**Fig. 3**). Gelatin zymography using different protein concentrations of tissue homogenate of uterus, placenta and aorta of RUPP rats showed similar concentration-dependent increases in proteolytic activity at 0.1, 0.2 and o.5 μg, clearly discernible bands at 1 to 2 μg, and almost saturated bands at 5 and 10 μg (**Fig. 3B, 3D, 3F**). The protein concentration-gelatinase activity curves were reduced in tissues of RUPP compared with Norm-Preg rats (**Fig. 3**). However, these assays were performed in different gels, and it was important to compare the MMPs gelatinase activity of tissues from Norm-Preg and RUPP rats in the same gel. Because 1 μg protein produced clearly discernible bands, all further gelatin zymography experiments comparing uterus, placenta and aorta of Norm-Preg and RUPP rats were performed using 1 μg protein for loading.

Gelatin zymography revealed that the gelatinase activity corresponding to pro-MMP-2, MMP-2, and pro-MMP-9 was reduced in uterus (**Fig. 4A**), placenta (**Fig. 4B**) and aorta (**Fig. 4C**) of RUPP vs. Norm-Preg rats. Also, the gelatinase activity of MMP-9 was significantly reduced in uterus (**Fig. 4A**) and aorta (**Fig. 4C**), and insignificantly reduced in placenta (**Fig. 4B**) of RUPP vs. Norm-Preg rats. The zymography data also showed a consistent gelatinolytic band at ~74 kDa adjacent to the pro-MMP-2 band. The nature of this band is unclear, but its intensity appeared to follow the same pattern as pro-MMP-2 (see Fig. 3 and 4). Quantitative analysis of this putative 74 kDa band in Fig. 4 indicated that its integrated density relative to actin in the uterus, placenta and aorta was significantly reduced in RUPP (1.45±0.19, 1.41±0.18, and 0.90±0.13, respectively) compared with Norm-Preg rats (2.68±0.34, 2.31±0.37, and 1.78±0.15, respectively). The zymography data also showed that MMP-2 was less than pro-MMP-2 in the uterus, placenta and aorta of both Norm-Preg and RUPP rats (**Fig. 4**), which is different from the Western blot data demonstrating that the amount of MMP-2 was greater than pro-MMP-2 in tissues of Norm-Preg and RUPP rats (see **Fig. 2**). On the other hand, the gelatinase activity of MMP-9 was comparable to pro-MMP-9 in uterus and aorta, but markedly less than pro-MMP-9 in the placenta of both Norm-Preg and RUPP rats, (**Fig. 4**). These zymography data are different from the Western blot data demonstrating that the amount of MMP-9 was less than pro-MMP-9 in the three tissues of Norm-Preg and RUPP rats (see **Fig. 2**). However, in both methods, the MMP-2/pro-MMP-2 and MMP-9/pro-MMP-9 ratios in the uterus, placenta or aorta were not significantly different in RUPP vs. Norm-Preg rats (**Fig. 2, 4**).

The pregnancy-associated changes in tissue structure and MMPs distribution were then examined using histology and immunohistochemistry. Because the pregnant rat uterus and placenta are large, only a small portion of the tissue section could be imaged even when using a 4× objective. Also, the uterine wall thickness was not homogeneous (**Fig. 5**). To circumvent this difficulty, and to perform quantitative analysis in the whole tissue section,

10 to 16 picture frames of sequential parts of the uterine tissue section were acquired using 4× objective, and the composite image of the whole uterine section was reconstituted and analyzed (**Fig. 5**). Similar procedure was followed to obtain composite image of the whole placenta tissue section.

Quantitative morphometry of H&E stained uterine sections showed reduction in the total area and wall area in RUPP vs. Norm-Preg rats (**Fig. 6A, 6B, 6C, 6D**). Immunohistochemical analysis revealed MMP-2 and MMP-9 brown staining in uterine sections of Norm-Preg (**Fig. 6A**) and RUPP rats (**Fig. 6B**). Quantitative image analysis showed that the brown staining for MMP-2 and MMP-9 was less in uterus of RUPP than Norm-Preg rats (**Fig. 6E, 6F**).

In the placenta, H&E staining and quantitative morphometry showed that the placenta central thickness and total cross-sectional area were less in RUPP than Norm-Preg rats (**Fig. 7A, 7B, 7C, 7D**). Immunohistochemistry revealed that MMP-2 and MMP-9 immunostaining was less in the placenta of RUPP than Norm-Preg rats (**Fig. 7A, 7B, 7E, 7F**).

H&E staining of the aorta showed insignificant decrease in total wall thickness (**Fig. 8A, 8D**), and no significant difference in the relative thickness of the intima, media and adventitia (**Fig. 8G**) in RUPP vs. Norm-Preg rats. Immunohistochemistry revealed less MMP-2 in the aorta of RUPP than Norm-Preg rats (**Fig. 8B, 8E**), and the reduction was more apparent in the media compared to other layers of the vascular wall (**Fig. 8H**). Similarly, MMP-9 immunostaining was less in aortic sections, particularly in aortic media of RUPP compared with Norm-Preg rats (**Fig. 8C, 8F, 8I**).

In all tissues tested, collagen staining could be detected and was more abundant in tissue sections of the uterus (**Fig. 9A, 9B**), placenta (**Fig. 9C, 9D**) and aorta (**Fig. 9E, 9F**) of RUPP than Norm-Preg rats (**Fig. 9G**). In comparison, elastin staining was sparse and diffuse in the uterus (**Fig. 10A, 10B**) and placenta (**Fig. 10C, 10D**) of Norm-Preg and RUPP rats. On the other hand, elastin staining was strong and well-defined in the aorta of Norm-Preg and RUPP rats (**Fig. 10E, 10F**). Nevertheless, quantitative analysis of the black staining indicated no significant difference in elastin content in the uterus, placenta or aorta of RUPP compared with Norm-Preg rats (**Fig. 10G**).

To test the effects of growth modulators, the protein amount of pro-MMP-2, MMP-2, pro-MMP-9 and MMP-9 was significantly reduced in uterus (**Fig. 11A**), placenta (**Fig. 11B**) and aorta (**Fig. 11C**) isolated from Norm-Preg rats and treated with sFlt-1 (0.1 μg/ml) in organ culture for 48 hr. In tissues of Norm-Preg rats treated with sFlt-1 plus VEGF (0.1 μg/ml) for 48 hr, no significant reduction in the amount of MMP-2 or MMP-9 was observed (**Fig. 11**). Also, in uterus, placenta and aorta isolated from RUPP rats and treated with VEGF, the amount of MMP-2 and MMP-9 was not significantly different from that in control Norm-Preg rats (**Fig. 11**), and was enhanced when compared to that in non-treated RUPP tissues (see **Fig. 2**).

Gelatin zymography showed that the gelatinase activity corresponding to pro-MMP-2, MMP-2, and pro-MMP-9 was significantly reduced in uterus (**Fig. 12A**), placenta (**Fig.**

12B) and aorta (**Fig. 12C**) isolated from Norm-Preg rats and treated with sFlt-1 for 48 hr in organ culture. Also, MMP-9 gelatinase activity was significantly reduced in uterus (**Fig. 12A**) and aorta (**Fig. 12C**), and insignificantly reduced in placenta (**Fig. 12B**) isolated from Norm-Preg rats and treated with sFlt-1 for 48 hr in organ culture. In tissues of Norm-Preg rats treated with sFlt-1 plus VEGF for 48 hr, the gelatinase activity was not significantly different from that in non-treated tissues of Norm-Preg rats (**Fig. 12**). Also, in isolated uterus, placenta and aorta of RUPP rats treated with VEGF for 48 hr, the MMP-2 and -9 gelatinase activity was not significantly different from that in Norm-Preg rats (**Fig. 12**), and was enhanced when compared to that in non-treated RUPP tissues (see **Fig. 4**).

4. Discussion

The main findings of the present study are: 1) Maternal BP is increased, uterine, placental and aortic tissue weight and cross-sectional area are decreased, and fetal litter size and pup weight are decreased in RUPP model of HTN-Preg compared with Norm-Preg rats, 2) MMP-2 and -9 expression/activity are reduced in uterus, placenta and aorta of RUPP vs. Norm-Preg rats, 3) Collagen, but not elastin, is increased in uterus, placenta and aorta of RUPP vs. Norm-Preg rats, and 4) The anti-angiogenic factor sFlt-1 decreases MMPs expression/activity in uterus, placenta and aorta of Norm-Preg rats, and the angiogenic factor VEGF reverses the effects of sFlt-1 in tissues of Norm-Preg rats and the decreases in MMP expression/activity in tissues of RUPP rats.

Preeclampsia is a complication of pregnancy with unclear mechanisms. Because of the difficulty to perform mechanistic studies in pregnant women, animal models of HTN-Preg have been developed [24, 25, 31-33]. RUPP during late pregnancy in sheep, dog, rabbit and rat induces a hypertensive state that closely resembles preeclampsia [24, 25]. Consistent with previous reports [34, 35], the present study showed that BP was increased, and the litter size and individual pup weight were decreased in RUPP vs. Norm-Preg rats. Importantly, the total body weight including uterus, placentae and pups was less in RUPP than Norm-Preg rats; however, the weight difference disappeared when the uterus with the placentae and pups were removed, suggesting growth-restrictive remodeling in the uterus and placenta of RUPP rats.

We further examined the specific changes in three important tissues during pregnancy; the uterus which undergoes remodeling to accommodate the growing fetus, the placenta which provides nutrient supply to the developing fetus, and the aorta for the vascular changes in the maternal circulation. The uterus, placenta, and aortic tissue weight was reduced in RUPP rats. Also, histological morphometry showed significant reduction in uterine and placental cross-sectional area, and insignificant reduction in aortic cross-sectional area in RUPP vs. Norm-Preg rats, supporting growth-restrictive remodeling in the uterus, placenta and vasculature of RUPP rats.

In search for the mechanisms involved in the changes in uteroplacental and vascular remodeling, Western blots and gelatin zymography revealed that MMP-2 and -9 were abundantly expressed and showed prominent gelatinase activity in tissues of Norm-Preg rats. Immunohistochemical analysis confirmed prominent MMP-2 and -9 immunostaining in

the uterus, placenta and aorta of Norm-Preg rats. These findings are consistent with previous reports [22] and support a role of MMPs in the uteroplacental and vascular remodeling associated with Norm-Preg. Importantly, MMPs immunostaining was particularly apparent in the aortic media, consistent with reports that vascular smooth muscle cells (VSMCs) are a major source of MMPs [36, 37].

In comparison with Norm-Preg rats, the uterus, placenta and aorta of RUPP rats appeared to have less MMP-2 and MMP-9 because: 1) Western blots revealed decreased protein amount of MMP-2 and MMP-9 in tissues of RUPP rats. 2) MMP-2 and MMP-9 gelatinase activity was reduced in tissues of RUPP rats. Further analysis of the ratio of MMP to pro-MMP forms as an estimate of the relative MMP activity in the tested tissues indicated that the MMP-2/pro-MMP-2 ratio in the uterus, placenta and aorta from either Norm-Preg or RUPP rats was >1 in the Western blots and <1 in the zymography studies. Also, MMP-9/pro-MMP-9 ratio in the uterus, placenta and aorta from either Norm-Preg or RUPP rats was <1 in the Western blots, and was ~1 in the uterus and aorta and was markedly reduced and reached ~0.1 in the placenta in the zymography studies. The cause of these differences is unclear but could be related to specific changes in MMP activity in the placenta as compared to other maternal tissues. This is supported by previous reports of tissue-specific changes in MMP activity in the placenta as compared to the uterus and aorta of late-Preg vs. mid-Preg rats [22]. Nevertheless, in both the Western blot and zymography experiments the MMP-2/Pro-MMP-2 and MMP-9/pro-MMP-9 ratios in all tissues tested were not significantly different in RUPP compared with Norm-Preg rats, supporting that the observed decreases in the amount/activity of MMP-2 and MMP-9 in RUPP rats are not due to relative changes in the cleaved vs. uncleaved form, but rather due a decrease in the total amount of the respective MMP. 3) MMP-2 and MMP-9 immunostaining was also reduced in uterine and placenta tissue sections and less intense in the aortic media of RUPP vs. Norm-Preg rats. The decreases in MMPs expression/activity, in parallel with the decreases in uterine, placental, and aortic tissue weight and cross-sectional area suggest a role for reduced MMPs expression/activity in growth-restrictive remodeling in tissues of RUPP rats.

To search for the downstream targets linking the changes in MMPs to the growth-restrictive tissue remodeling, we investigated possible changes in MMPs substrates. MMPs degrade different substrates including gelatin, collagen, and other proteins [14, 15, 38]. Picro-Sirius Red staining revealed an increase in collagen content in uterus, placenta and aorta of RUPP compared with Norm-Preg rats. Because MMPs facilitate cell growth and migration by promoting proteolysis of ECM, the decreased MMPs and increased collagen deposition in RUPP tissues could impede smooth muscle cell growth, proliferation and migration, and thus interfere with uteroplacental tissue invasion and decrease uterine and placental growth. Also, while the aortic collagen content increased there was a significant decrease in aortic tissue weight and insignificant decrease in aortic thickness in RUPP rats, likely because the decreased MMPs and increased collagen content would interfere with VSMC growth. This is supported by reports that upregulation of MMP-1 enhances flow-induced VSMC motility in cell culture, and MMP-1 inhibition attenuates flow-induced migration [39]. Also, MMP-2 knockout (KO) is associated with decreased VSMC migration and neointima formation in the mouse carotid ligation model [40, 41]. Additionally, MMP-9 KO is associated with reduced VSMC migration and neointima formation in mouse carotid occlusion model [42],

and reduces VSMC migration and proliferation and neointima formation in mouse model of carotid artery injury [43]. The decreased MMPs activity and increased vascular collagen content could also increase vessel rigidity and decrease its plasticity and thus contributes to increased vascular resistance and HTN. This is consistent with reports that MMP-1, -2, and -9 gelatinolytic activity is decreased and collagen deposition is increased in internal mammary artery from hypertensive compared with normotensive patients undergoing coronary artery bypass surgery [44]. Angiotensin II infusion and high salt diet in mice are also associated with HTN and increased MMP-9 activity in carotid artery, and MMP-9 KO is associated with vessel stiffness and increased pulse pressure, suggesting a beneficial role of MMP-9 in preserving vessel compliance and alleviating the increase in BP in early HTN [45]. Also, in adult spontaneously hypertensive rat, a decrease in MMP-1, -2, and -3 may contribute to remodeling of resistance arteries and the setting of HTN [46]. It is important to note that collagen has 18 types and different subtypes [47], and MMP-2 can degrade collagen I, II, III, IV, V, VII, X, and XI while MMP-9 can degrade collagen IV, V, VII, X, XIV [14, 15, 38]. Future Western blot and immunohistochemistry studies should measure the changes in the various collagen types and subtypes in HTN-Preg. RT-PCR experiments should also determine whether any increases in a specific collagen type or subtype are solely due to decreased degradation or could also involve decreased *de novo* collagen mRNA expression and protein biosynthesis.

In contrast with collagen, elastin is less likely to be involved in the observed changes in tissue growth and remodeling because elastin staining of uterus and placenta was sparse and diffuse and not different in RUPP vs. Norm-Preg rats. Although prominent and well-defined elastin bands could be observed in the aorta, no significant changes were noted between RUPP and Norm-Preg rats, suggesting little role of elastin in the observed changes in aortic growth and remodeling.

In addition to their proteolytic effects on ECM proteins, MMPs may also affect uterine and vascular function and the mechanisms of smooth muscle contraction. We have shown that MMP-2 and -9 cause relaxation of precontracted rat uterus [21], aorta [30], and inferior vena cava [48, 49]. Thus the decrease in uterine MMPs expression/activity could lead to increased uterine contraction and premature labor. Also, the decrease in vascular MMPs expression/activity could lead to increased vascular contraction and HTN-Preg. This is consistent with previous reports that vascular contraction is enhanced in RUPP rats [25].

We also searched for the upstream mechanisms linking placental ischemia to the changes in MMPs expression/activity, and examined the effects of potential factors released during the course of preeclampsia and HTN-Preg. Studies in preeclamptic women have shown an imbalance between the pro-angiogenic factors VEGF and PlGF, and the anti-angiogenic factor sFlt-1 [13, 50-58]. Also, experimental studies showed that placental ischemia in RUPP rats is associated with increased serum sFlt-1 [12] and sEng [13], and that infusion or adenoviral overexpression of sFlt-1 in Norm-Preg rats results in increased BP and decreased plasma VEGF [58-60]. These observations led to the suggestion that sFlt-1 could cause generalized endotheliosis in blood vessels leading to HTN, in the glomeruli leading to proteinuria, and in brain vessels leading to seizures and eclampsia [60]. However, in these *in vivo* sFlt-1 infusion experiments it is often difficult to determine if any observed effects are

caused directly by sFlt-1 or involve a cascade of biochemical events and other mediators and pathways, and therefore the direct targets of sFlt-1 have not been clearly defined. Specifically, little information is available on whether sFlt-1 could target tissue MMPs particularly during pregnancy. Some studies have shown that sFlt-1-induced inhibition of VEGFR2 decreases visfatin-induced endothelial VEGF production and MMP-2 and -9 expression/activity [61]. Other studies in mouse model of abdominal aortic aneurysm have shown that treatment with sFlt-1 reduces aneurysm size and attenuates MMP-2 and -9 activity in periaortic tissue [62]. The present study supports a role of sFlt-1 as a potential upstream mechanism linking placental ischemia to the decrease in MMPs in HTN-Preg because: 1) sFlt-1 reduced MMPs amount/activity in uterine, placental and vascular tissues of Norm-Preg rats, 2) VEGF reversed the sFlt-1 induced decreases in MMPs amount/activity in tissues of Norm-Preg rats, and 3) VEGF increased MMPs levels in tissues of RUPP rats to levels similar to those observed in Norm-Preg rats. These observations are consistent with the report that infusion of the pro-angiogenic factor VEGF reduces BP in RUPP rats [63]. Angiogenic growth factors such as VEGF and TGF-β are secreted by endothelial cells and other cells and act in an autocrine or paracrine fashion to accelerate angiogenesis, and MMPs may mediate these effects by virtue of their proteolytic activity and other mechanisms including helping to detach pericytes from the vessels undergoing angiogenesis, releasing ECM-bound angiogenic growth factors, exposing cryptic pro-angiogenic integrin binding sites in the ECM, generating pro-migratory ECM component fragments, and cleaving endothelial cell-cell adhesions [64]. This is supported by reports that MMP-1, -3, -7, -8, -9, -10, -13, and -19 expression is upregulated in human umbilical vein endothelial cells treated with VEGF, and that VEGF induces MMP-10 expression via PI_3K and MAPK pathways [65]. Also, trophoblast- and VSM-derived MMP-12 could mediate proteolysis and uterine spiral artery remodeling during pregnancy [66].

We should note that MMPs is a large family of at least 28 proteolytic enzymes [14, 15, 38]. While the present study examined the changes in MMP-2 and -9, other MMPs have been detected in the uterus, placenta and aorta, and the changes in these MMPs in HTN-Preg need to be investigated. Importantly, MMPs activity could be influenced by other MMP activators and inhibitors. For example, some MMPs may cleave other pro-MMPs, and membrane-type (MT)1-MMP is a key activator of pro-MMP-2 [14, 15, 38, 67]. On the other hand, tissue inhibitors of MMPs (TIMP-1 and TIMP-2) are endogenous modulators of MMPs activity [14, 15, 38, 67], and the changes in their expression/activity in HTN-Preg need to be examined. Also, in the present study the changes in uterine, placental and aortic MMPs were measured at day 19 of gestation, and the progressive changes during the course of pregnancy and their reversal in the postpartum period need to be examined. Plasma levels of MMPs have also been shown to increase during pregnancy [68], suggesting a role for MMPs in different maternal tissues. Instead of measuring plasma MMPs levels, which often reflect global changes in multiple tissues, the present study focused on examining three important pregnancy-relevant tissues. While we were able to detect significant changes in uterine, placental and aortic MMPs in HTN-Preg rats, that should not minimize the importance of measuring the structural changes and MMPs expression in other tissues particularly the small resistance vessels which affect BP. Another limitation is that RUPP during pregnancy may cause the release of not only anti-angiogenic factors, but also other vasoactive factors

including cytokines, reactive oxygen species and hypoxia-inducible factors, which could in turn lead to uteroplacental and vascular dysfunction during HTN-Preg [6, 12, 13, 32, 33, 69, 70]. Interestingly, cytokines, reactive oxygen species and hypoxia-inducible factors have been shown to affect MMPs expression/activity [71, 72], and studying their differential effects as well as the effects of their inhibitors on MMPs activity in Norm-Preg and HTN-Preg should be examined in future investigations.

In conclusion, HTN-Preg is associated with decreased uterine, placental and aortic tissue weight and cross sectional area, decreased expression/activity of MMP-2 and -9, and increased collagen content, suggesting a role for MMPs in growth-restrictive remodeling in HTN-Preg. Anti-angiogenic factors such as sFlt-1 decrease MMPs expression/activity in uterus, placenta and aorta of Norm-Preg rats, and the angiogenic factor VEGF reverses the effects of sFlt-1 in tissues of Norm-Preg rats and the decreases in MMPs expression/activity in tissues of RUPP rats. Targeting MMPs could provide a new approach for the detection and management of HTN-Preg and preeclampsia.

Supplementary Material

Refer to Web version on PubMed Central for supplementary material.

Acknowledgments

This work was supported by grants from National Heart, Lung, and Blood Institute (HL-65998, HL-98724, HL-111775) and The Eunice Kennedy Shriver National Institute of Child Health and Human Development (HD-60702). Dr. W. Li was a visiting scholar from Tongji Hospital, Huazhong University of Science & Technology, Wuhan, Hubei Province, P.R. China, and a recipient of scholarship from the China Scholarship Council. We thank Tachianna Griffiths, Rachel Kana and Emily Jiang for their assistance in preparing the tissue samples, and with the data and image acquisition and analysis.

List of Abbreviations

BP	blood pressure
ECM	extracellular matrix
HTN	hypertension
HTN Preg	hypertensive-pregnancy
KO	knockout
MMP	matrix metalloproteinase
Norm-Preg	normal pregnant
PlGF	placental growth factor
RUPP	reduced uteroplacental perfusion pressure
sEng	soluble endoglin
sFlt-1	soluble fms-like tyrosine kinase-1
VEGF	vascular endothelial growth factor

VSM vascular smooth muscle

References

1. Ouzounian JG, Elkayam U. Physiologic changes during normal pregnancy and delivery. Cardiol Clin. 2012; 30:317–29. [PubMed: 22813360]
2. Majed BH, Khalil RA. Molecular mechanisms regulating the vascular prostacyclin pathways and their adaptation during pregnancy and in the newborn. Pharmacol Rev. 2012; 64:540–82. [PubMed: 22679221]
3. Mandala M, Osol G. Physiological remodelling of the maternal uterine circulation during pregnancy. Basic Clin Pharmacol Toxicol. 2012; 110:12–8. [PubMed: 21902814]
4. Valdes G, Corthorn J. Review: The angiogenic and vasodilatory utero-placental network. Placenta. 2011; 32(Suppl 2):S170–5. [PubMed: 21295852]
5. Khalil RA, Granger JP. Vascular mechanisms of increased arterial pressure in preeclampsia: lessons from animal models. Am J Physiol Regul Integr Comp Physiol. 2002; 283:R29–45. [PubMed: 12069928]
6. Reslan OM, Khalil RA. Molecular and vascular targets in the pathogenesis and management of the hypertension associated with preeclampsia. Cardiovasc Hematol Agents Med Chem. 2010; 8:204–26. [PubMed: 20923405]
7. Palei AC, Spradley FT, Warrington JP, George EM, Granger JP. Pathophysiology of hypertension in pre-eclampsia: a lesson in integrative physiology. Acta Physiol (Oxf). 2013; 208:224–33. [PubMed: 23590594]
8. Roberts JM, Gammill HS. Preeclampsia: recent insights. Hypertension. 2005; 46:1243–9. [PubMed: 16230510]
9. Uzan J, Carbonnel M, Piconne O, Asmar R, Ayoubi JM. Pre-eclampsia: pathophysiology, diagnosis, and management. Vasc Health Risk Manag. 2011; 7:467–74. [PubMed: 21822394]
10. Khalil RA, Crews JK, Novak J, Kassab S, Granger JP. Enhanced vascular reactivity during inhibition of nitric oxide synthesis in pregnant rats. Hypertension. 1998; 31:1065–9. [PubMed: 9576115]
11. Levine RJ, Maynard SE, Qian C, Lim KH, England LJ, Yu KF, et al. Circulating angiogenic factors and the risk of preeclampsia. N Engl J Med. 2004; 350:672–83. [PubMed: 14764923]
12. Gilbert JS, Babcock SA, Granger JP. Hypertension produced by reduced uterine perfusion in pregnant rats is associated with increased soluble fms-like tyrosine kinase-1 expression. Hypertension. 2007; 50:1142–7. [PubMed: 17923588]
13. Gilbert JS, Gilbert SA, Arany M, Granger JP. Hypertension produced by placental ischemia in pregnant rats is associated with increased soluble endoglin expression. Hypertension. 2009; 53:399–403. [PubMed: 19075097]
14. Visse R, Nagase H. Matrix metalloproteinases and tissue inhibitors of metalloproteinases: structure, function, and biochemistry. Circ Res. 2003; 92:827–39. [PubMed: 12730128]
15. Raffetto JD, Khalil RA. Matrix metalloproteinases and their inhibitors in vascular remodeling and vascular disease. Biochem Pharmacol. 2008; 75:346–59. [PubMed: 17678629]
16. Moreira L, de Carvalho EC, Caldas-Bussiere MC. Differential immunohistochemical expression of matrix metalloproteinase-2 and tissue inhibitor of metalloproteinase-2 in cow uteri with adenomyosis during follicular phase. Vet Res Commun. 2011; 35:261–9. [PubMed: 21626345]
17. Kizaki K, Ushizawa K, Takahashi T, Yamada O, Todoroki J, Sato T, et al. Gelatinase (MMP-2 and -9) expression profiles during gestation in the bovine endometrium. Reprod Biol Endocrinol. 2008; 6:66. [PubMed: 19116037]
18. Ulbrich SE, Meyer SU, Zitta K, Hiendleder S, Sinowatz F, Bauersachs S, et al. Bovine endometrial metallopeptidases MMP14 and MMP2 and the metallopeptidase inhibitor TIMP2 participate in maternal preparation of pregnancy. Mol Cell Endocrinol. 2011; 332:48–57. [PubMed: 20887771]
19. Mishra B, Kizaki K, Koshi K, Ushizawa K, Takahashi T, Hosoe M, et al. Expression of extracellular matrix metalloproteinase inducer (EMMPRIN) and its related extracellular matrix

degrading enzymes in the endometrium during estrous cycle and early gestation in cattle. Reprod Biol Endocrinol. 2010; 8:60. [PubMed: 20540754]

20. Zhang X, Qi C, Lin J. Enhanced expressions of matrix metalloproteinase (MMP)-2 and -9 and vascular endothelial growth factors (VEGF) and increased microvascular density in the endometrial hyperplasia of women with anovulatory dysfunctional uterine bleeding. Fertil Steril. 2010; 93:2362–7. [PubMed: 19249761]
21. Yin Z, Sada AA, Reslan OM, Narula N, Khalil RA. Increased MMPs expression and decreased contraction in the rat myometrium during pregnancy and in response to prolonged stretch and sex hormones. Am J Physiol Endocrinol Metab. 2012; 303:E55–70. [PubMed: 22496348]
22. Dang Y, Li W, Tran V, Khalil RA. EMMPRIN-mediated induction of uterine and vascular matrix metalloproteinases during pregnancy and in response to estrogen and progesterone. Biochem Pharmacol. 2013; 86:734–47. [PubMed: 23856290]
23. Anderson CM, Lopez F, Zhang HY, Shirasawa Y, Pavlish K, Benoit JN. Mesenteric vascular responsiveness in a rat model of pregnancy-induced hypertension. Exp Biol Med (Maywood). 2006; 231:1398–402. [PubMed: 16946408]
24. Alexander BT, Kassab SE, Miller MT, Abram SR, Reckelhoff JF, Bennett WA, et al. Reduced uterine perfusion pressure during pregnancy in the rat is associated with increases in arterial pressure and changes in renal nitric oxide. Hypertension. 2001; 37:1191–5. [PubMed: 11304523]
25. Crews JK, Herrington JN, Granger JP, Khalil RA. Decreased endothelium-dependent vascular relaxation during reduction of uterine perfusion pressure in pregnant rat. Hypertension. 2000; 35:367–72. [PubMed: 10642326]
26. Chen W, Khalil RA. Differential [Ca2+]i signaling of vasoconstriction in mesenteric microvessels of normal and reduced uterine perfusion pregnant rats. Am J Physiol Regul Integr Comp Physiol. 2008; 295:R1962–72. [PubMed: 18843089]
27. Eder DJ, McDonald MT. A role for brain angiotensin II in experimental pregnancy-induced hypertension in laboratory rats. Clin Exp Hyper Hyper Preg. 1987; 6:431–51.
28. Stennett AK, Qiao X, Falone AE, Koledova VV, Khalil RA. Increased vascular angiotensin type 2 receptor expression and NOS-mediated mechanisms of vascular relaxation in pregnant rats. Am J Physiol Heart Circ Physiol. 2009; 296:H745–55. [PubMed: 19151255]
29. Whittaker P, Kloner RA, Boughner DR, Pickering JG. Quantitative assessment of myocardial collagen with picrosirius red staining and circularly polarized light. Basic Res Cardiol. 1994; 89:397–410. [PubMed: 7535519]
30. Chew DK, Conte MS, Khalil RA. Matrix metalloproteinase-specific inhibition of Ca2+ entry mechanisms of vascular contraction. J Vasc Surg. 2004; 40:1001–10. [PubMed: 15557917]
31. Losonczy G, Brown G, Venuto RC. Increased peripheral resistance during reduced uterine perfusion pressure hypertension in pregnant rabbits. Am J Med Sci. 1992; 303:233–40. [PubMed: 1562040]
32. Davis JR, Giardina JB, Green GM, Alexander BT, Granger JP, Khalil RA. Reduced endothelial NO-cGMP vascular relaxation pathway during TNF-alpha-induced hypertension in pregnant rats. Am J Physiol Regul Integr Comp Physiol. 2002; 282:R390–9. [PubMed: 11792648]
33. Orshal JM, Khalil RA. Reduced endothelial NO-cGMP-mediated vascular relaxation and hypertension in IL-6-infused pregnant rats. Hypertension. 2004; 43:434–44. [PubMed: 14707155]
34. Alexander BT, Cockrell K, Cline FD, Llinas MT, Sedeek M, Granger JP. Effect of angiotensin II synthesis blockade on the hypertensive response to chronic reductions in uterine perfusion pressure in pregnant rats. Hypertension. 2001; 38:742–5. [PubMed: 11566968]
35. Granger JP, Alexander BT, Llinas MT, Bennett WA, Khalil RA. Pathophysiology of preeclampsia: linking placental ischemia/hypoxia with microvascular dysfunction. Microcirculation. 2002; 9:147–60. [PubMed: 12080413]
36. Seo KW, Lee SJ, Kim YH, Bae JU, Park SY, Bae SS, et al. Mechanical stretch increases MMP-2 production in vascular smooth muscle cells via activation of PDGFR-beta/Akt signaling pathway. PLoS One. 2013; 8:e70437. [PubMed: 23950935]
37. Li HX, Kong FJ, Bai SZ, He W, Xing WJ, Xi YH, et al. Involvement of calcium-sensing receptor in oxLDL-induced MMP-2 production in vascular smooth muscle cells via PI3K/Akt pathway. Mol Cell Biochem. 2012; 362:115–22. [PubMed: 22083546]

38. Kucukguven A, Khalil RA. Matrix metalloproteinases as potential targets in the venous dilation associated with varicose veins. Curr Drug Targets. 2013; 14:287–324. [PubMed: 23316963]
39. Shi ZD, Ji XY, Berardi DE, Qazi H, Tarbell JM. Interstitial flow induces MMP-1 expression and vascular SMC migration in collagen I gels via an ERK1/2-dependent and c-Jun-mediated mechanism. Am J Physiol Heart Circ Physiol. 2010; 298:H127–35. [PubMed: 19880665]
40. Cheng XW, Kuzuya M, Sasaki T, Arakawa K, Kanda S, Sumi D, et al. Increased expression of elastolytic cysteine proteases, cathepsins S and K, in the neointima of balloon-injured rat carotid arteries. Am J Pathol. 2004; 164:243–51. [PubMed: 14695337]
41. Johnson C, Galis ZS. Matrix metalloproteinase-2 and -9 differentially regulate smooth muscle cell migration and cell-mediated collagen organization. Arterioscler Thromb Vasc Biol. 2004; 24:54–60. [PubMed: 14551157]
42. Galis ZS, Johnson C, Godin D, Magid R, Shipley JM, Senior RM, et al. Targeted disruption of the matrix metalloproteinase-9 gene impairs smooth muscle cell migration and geometrical arterial remodeling. Circ Res. 2002; 91:852–9. [PubMed: 12411401]
43. Cho A, Reidy MA. Matrix metalloproteinase-9 is necessary for the regulation of smooth muscle cell replication and migration after arterial injury. Circ Res. 2002; 91:845–51. [PubMed: 12411400]
44. Ergul A, Portik-Dobos V, Hutchinson J, Franco J, Anstadt MP. Downregulation of vascular matrix metalloproteinase inducer and activator proteins in hypertensive patients. Am J Hypertens. 2004; 17:775–82. [PubMed: 15363819]
45. Flamant M, Placier S, Dubroca C, Esposito B, Lopes I, Chatziantoniou C, et al. Role of matrix metalloproteinases in early hypertensive vascular remodeling. Hypertension. 2007; 50:212–8. [PubMed: 17515450]
46. Intengan HD, Schiffrin EL. Structure and mechanical properties of resistance arteries in hypertension: role of adhesion molecules and extracellular matrix determinants. Hypertension. 2000; 36:312–8. [PubMed: 10988257]
47. Gelse K, Poschl E, Aigner T. Collagens--structure, function, and biosynthesis. Adv Drug Deliv Rev. 2003; 55:1531–46. [PubMed: 14623400]
48. Raffetto JD, Barros YV, Wells AK, Khalil RA. MMP-2 induced vein relaxation via inhibition of [Ca2+]e-dependent mechanisms of venous smooth muscle contraction. Role of RGD peptides. J Surg Res. 2010; 159:755–64. [PubMed: 19482300]
49. Raffetto JD, Ross RL, Khalil RA. Matrix metalloproteinase 2-induced venous dilation via hyperpolarization and activation of K+ channels: relevance to varicose vein formation. J Vasc Surg. 2007; 45:373–80. [PubMed: 17264019]
50. Karumanchi SA, Bdolah Y. Hypoxia and sFlt-1 in preeclampsia: the “chicken-and-egg” question. Endocrinology. 2004; 145:4835–7. [PubMed: 15489315]
51. Wolf M, Shah A, Lam C, Martinez A, Smirnakis KV, Epstein FH, et al. Circulating levels of the antiangiogenic marker sFLT-1 are increased in first versus second pregnancies. Am J Obstet Gynecol. 2005; 193:16–22. [PubMed: 16021053]
52. Rajakumar A, Michael HM, Rajakumar PA, Shibata E, Hubel CA, Karumanchi SA, et al. Extra-placental expression of vascular endothelial growth factor receptor-1, (Flt-1) and soluble Flt-1 (sFlt-1), by peripheral blood mononuclear cells (PBMCs) in normotensive and preeclamptic pregnant women. Placenta. 2005; 26:563–73. [PubMed: 15993706]
53. Rana S, Karumanchi SA, Levine RJ, Venkatesha S, Rauh-Hain JA, Tamez H, et al. Sequential changes in antiangiogenic factors in early pregnancy and risk of developing preeclampsia. Hypertension. 2007; 50:137–42. [PubMed: 17515455]
54. Lam C, Lim KH, Karumanchi SA. Circulating angiogenic factors in the pathogenesis and prediction of preeclampsia. Hypertension. 2005; 46:1077–85. [PubMed: 16230516]
55. LaMarca BD, Gilbert J, Granger JP. Recent progress toward the understanding of the pathophysiology of hypertension during preeclampsia. Hypertension. 2008; 51:982–8. [PubMed: 18259004]
56. Tsatsaris V, Goffin F, Munaut C, Brichant JF, Pignon MR, Noel A, et al. Overexpression of the soluble vascular endothelial growth factor receptor in preeclamptic patients: pathophysiological consequences. J Clin Endocrinol Metab. 2003; 88:5555–63. [PubMed: 14602804]

57. Makris A, Thornton C, Thompson J, Thomson S, Martin R, Ogle R, et al. Uteroplacental ischemia results in proteinuric hypertension and elevated sFLT-1. Kidney Int. 2007; 71:977–84. [PubMed: 17377512]
58. Maynard SE, Min JY, Merchan J, Lim KH, Li J, Mondal S, et al. Excess placental soluble fms-like tyrosine kinase 1 (sFlt1) may contribute to endothelial dysfunction, hypertension, and proteinuria in preeclampsia. J Clin Invest. 2003; 111:649–58. [PubMed: 12618519]
59. Bridges JP, Gilbert JS, Colson D, Gilbert SA, Dukes MP, Ryan MJ, et al. Oxidative stress contributes to soluble fms-like tyrosine kinase-1 induced vascular dysfunction in pregnant rats. Am J Hypertens. 2009; 22:564–8. [PubMed: 19265787]
60. Li Z, Zhang Y, Ying Ma J, Kapoun AM, Shao Q, Kerr I, et al. Recombinant vascular endothelial growth factor 121 attenuates hypertension and improves kidney damage in a rat model of preeclampsia. Hypertension. 2007; 50:686–92. [PubMed: 17724276]
61. Adya R, Tan BK, Punn A, Chen J, Randeva HS. Visfatin induces human endothelial VEGF and MMP-2/9 production via MAPK and PI3K/Akt signalling pathways: novel insights into visfatin-induced angiogenesis. Cardiovasc Res. 2008; 78:356–65. [PubMed: 18093986]
62. Kaneko H, Anzai T, Takahashi T, Kohno T, Shimoda M, Sasaki A, et al. Role of vascular endothelial growth factor-A in development of abdominal aortic aneurysm. Cardiovasc Res. 2011; 91:358–67. [PubMed: 21436157]
63. Gilbert JS, Verzwyvelt J, Colson D, Arany M, Karumanchi SA, Granger JP. Recombinant vascular endothelial growth factor 121 infusion lowers blood pressure and improves renal function in rats with placentalischemia-induced hypertension. Hypertension. 2010; 55:380–5. [PubMed: 20026764]
64. Pepper MS. Extracellular proteolysis and angiogenesis. Thromb Haemost. 2001; 86:346–55. [PubMed: 11487024]
65. Heo SH, Choi YJ, Ryoo HM, Cho JY. Expression profiling of ETS and MMP factors in VEGF-activated endothelial cells: role of MMP-10 in VEGF-induced angiogenesis. J Cell Physiol. 2010; 224:734–42. [PubMed: 20432469]
66. Harris LK, Smith SD, Keogh RJ, Jones RL, Baker PN, Knofler M, et al. Trophoblast- and vascular smooth muscle cell-derived MMP-12 mediates elastolysis during uterine spiral artery remodeling. Am J Pathol. 2010; 177:2103–15. [PubMed: 20802175]
67. Pascual G, Rodriguez M, Gomez-Gil V, Trejo C, Bujan J, Bellon JM. Active matrix metalloproteinase-2 upregulation in the abdominal skin of patients with direct inguinal hernia. Eur J Clin Invest. 2010; 40:1113–21. [PubMed: 20718849]
68. Merchant SJ, Davidge ST. The role of matrix metalloproteinases in vascular function: implications for normal pregnancy and pre-eclampsia. BJOG. 2004; 111:931–9. [PubMed: 15327607]
69. LaMarca BB, Bennett WA, Alexander BT, Cockrell K, Granger JP. Hypertension produced by reductions in uterine perfusion in the pregnant rat: role of tumor necrosis factor-alpha. Hypertension. 2005; 46:1022–5. [PubMed: 16144982]
70. LaMarca BD, Ryan MJ, Gilbert JS, Murphy SR, Granger JP. Inflammatory cytokines in the pathophysiology of hypertension during preeclampsia. Curr Hypertens Rep. 2007; 9:480–5. [PubMed: 18367011]
71. Awad AE, Kandalam V, Chakrabarti S, Wang X, Penninger JM, Davidge ST, et al. Tumor necrosis factor induces matrix metalloproteinases in cardiomyocytes and cardiofibroblasts differentially via superoxide production in a PI3Kgamma-dependent manner. Am J Physiol Cell Physiol. 2010; 298:C679–92. [PubMed: 20007453]
72. Lim CS, Qiao X, Reslan OM, Xia Y, Raffetto JD, Paleolog E, et al. Prolonged mechanical stretch is associated with upregulation of hypoxia-inducible factors and reduced contraction in rat inferior vena cava. J Vasc Surg. 2011; 53:764–73. [PubMed: 21106323]

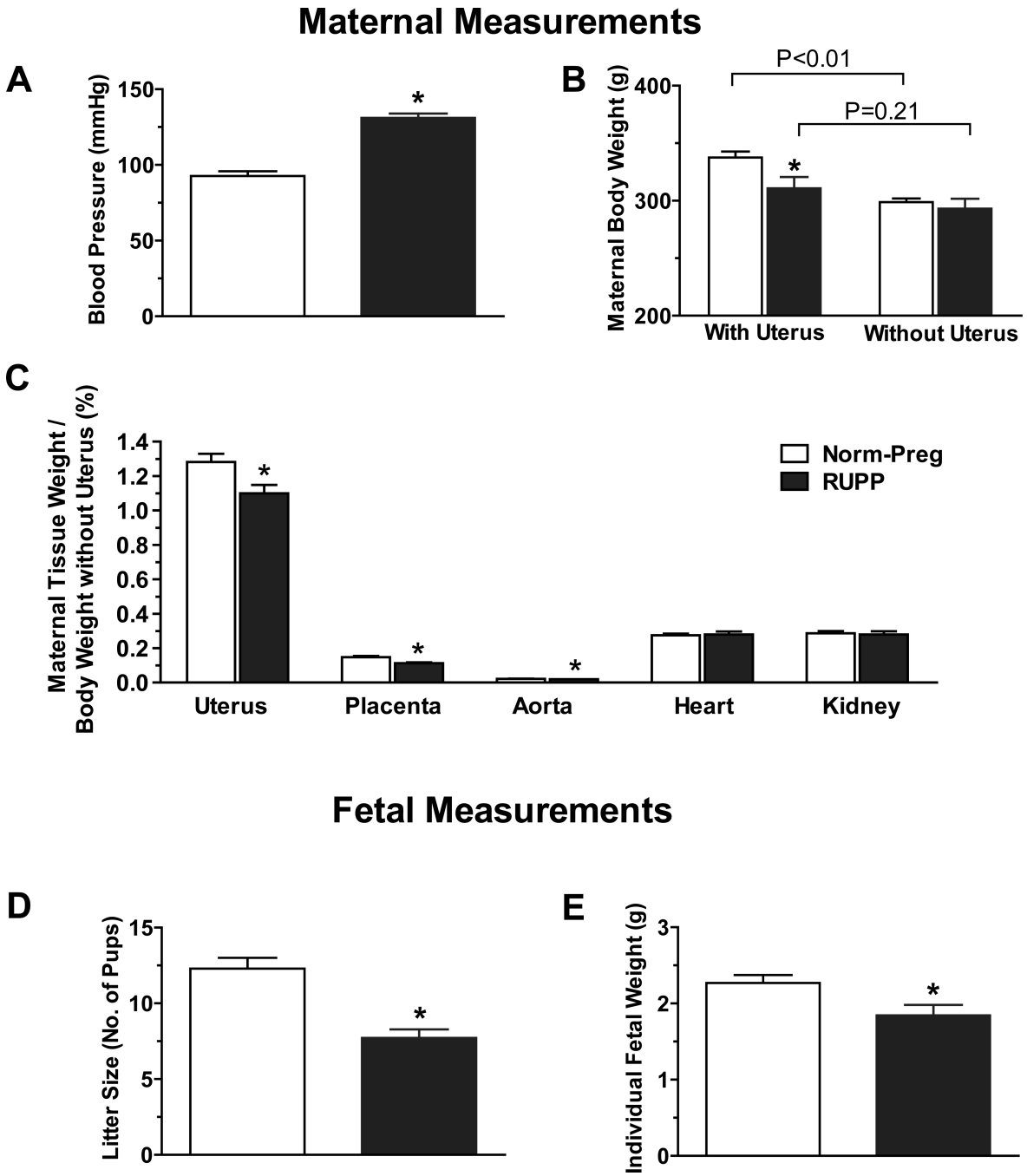

Fig. 1.

Maternal and fetal measurements in Norm-Preg and RUPP rats. On day 19 of pregnancy, BP (A) and body weight (B) were measured in Norm-Preg and RUPP rats. The animals were sacrificed and the whole uterus weight (without placentae or pups), average placenta weight, thoracic aorta, heart and average kidney weight were measured and presented as percentage of maternal body weight without uterus (C). Also, the pups were separated and the litter size (D) and average fetal weight (E) were measured. Bar graphs represent means±SEM, n = 6 to

7/group. * Measurements in RUPP rats are significantly different ($P<0.05$) from corresponding measurements in Norm-Preg rats.

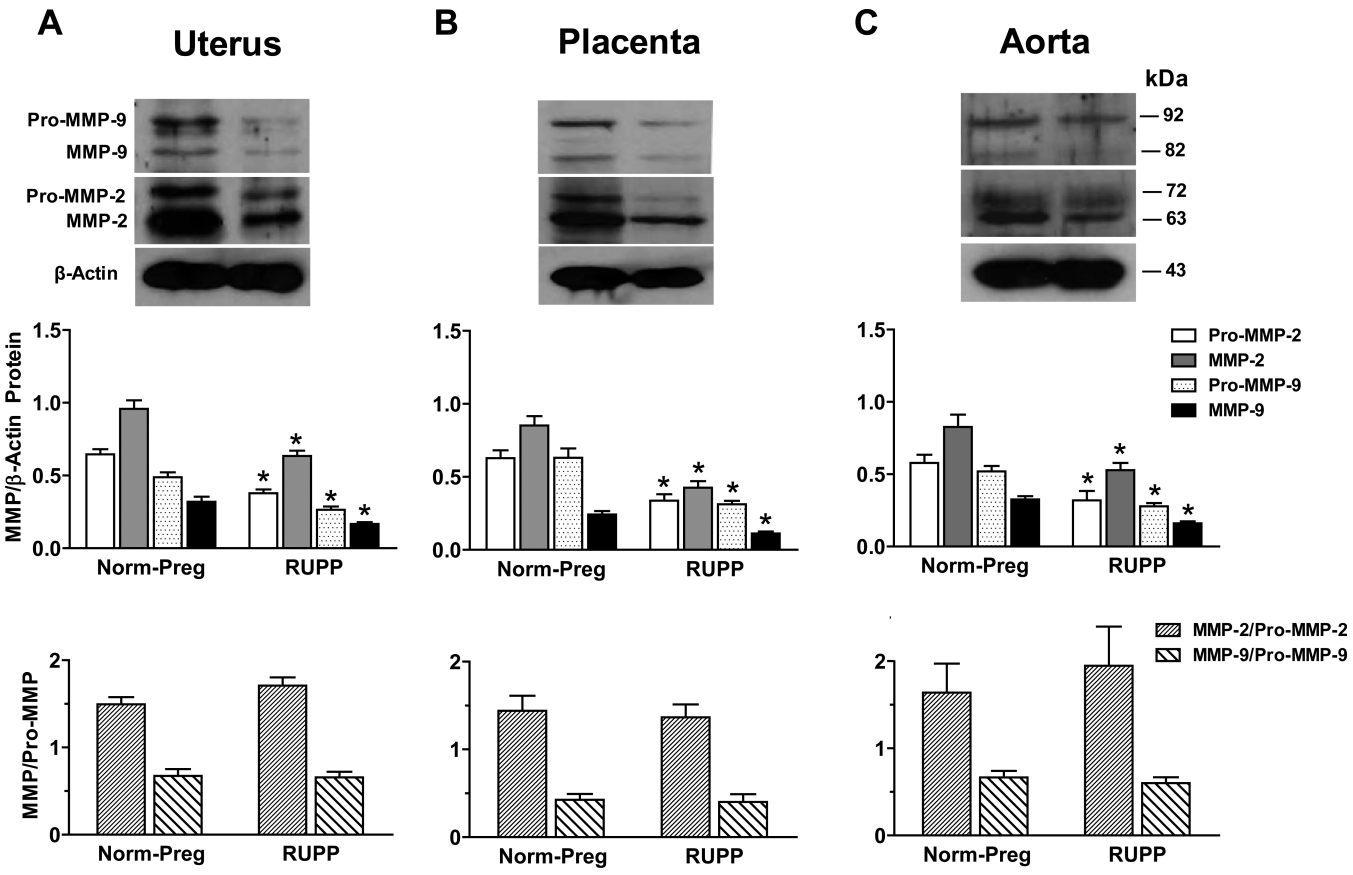

Fig. 2.

Protein amount of uterine, placental and aortic MMP-2 and MMP-9 in Norm-Preg and RUPP rats. Tissue homogenates of the uterus (A), placenta (B), and aorta (C) of Norm-Preg and RUPP rats were prepared for Western blot analysis using antibodies to MMP-2 (1:1000) and MMP-9 (1:1000). Immunoreactive bands corresponding to pro-MMP-2, MMP-2, pro-MMP-9 and MMP-9 were analyzed by optical densitometry and normalized to β-actin to correct for loading. The MMP-2/pro-MMP-2 and MMP-9/pro-MMP-9 ratios were also measured. Bar graphs represent means±SEM, n = 9/group. * Measurements in RUPP rats are significantly different ($P<0.05$) from corresponding measurements in Norm-Preg rats.

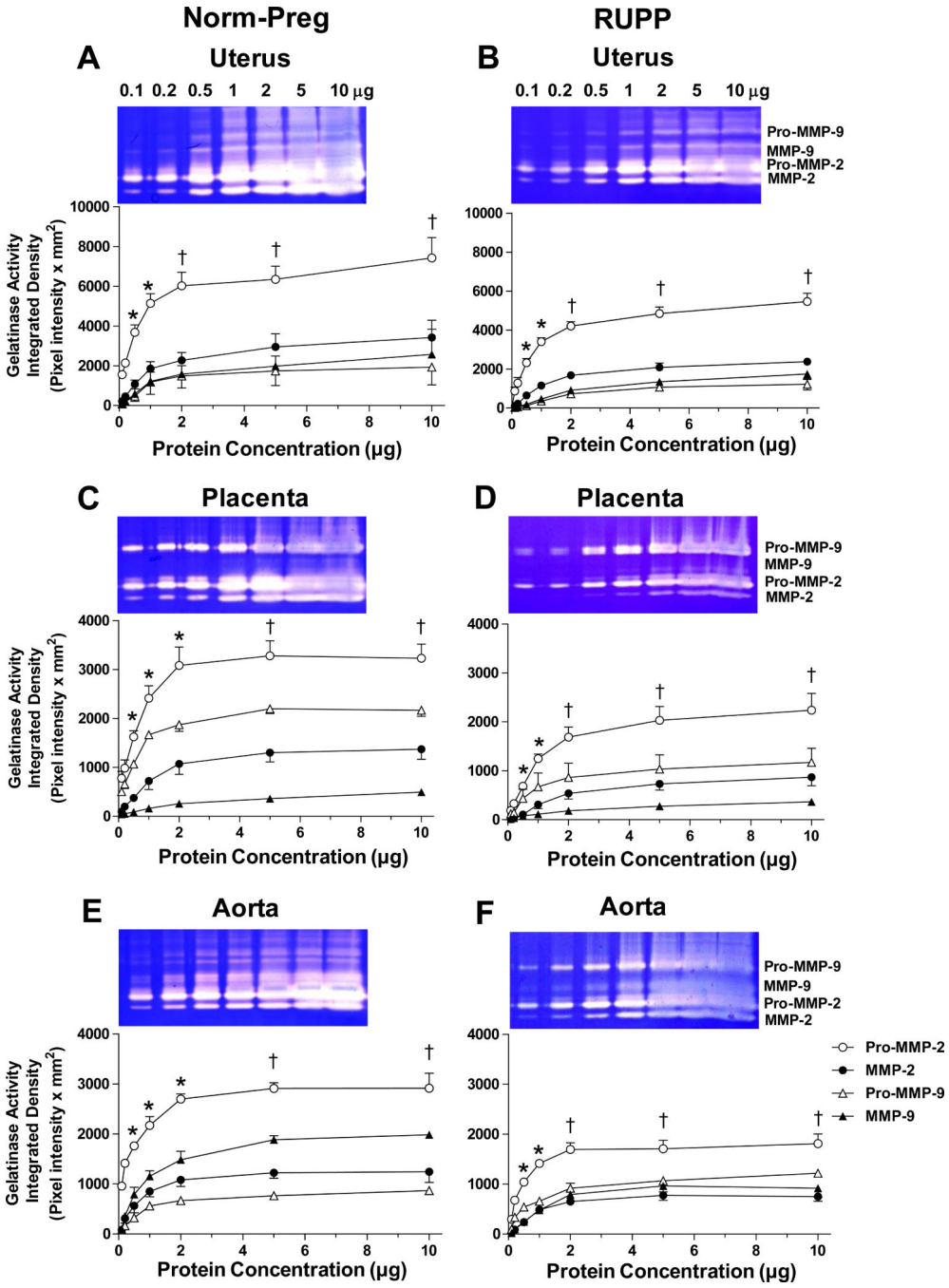

Fig. 3.

Concentration-dependent MMP-2 and MMP-9 gelatinase activity in uterus, placenta and aorta of Norm-Preg and RUPP rats. Uterine (A and B), placental (C and D) and aortic tissue strips (E and F) from Norm-Preg (A, C and E) and RUPP rats (B, D and F) were homogenized and prepared for gelatin zymography analysis using different concentrations of loaded protein (0.1 – 10 µg). The densitometry values of the proteolytic bands was presented as pixel intensity × mm^2. Line graphs represent means±SEM, n = 4/group. For pro-MMP-2, MMP-2, pro-MMP-9 and MMP-9, * Significantly different ($P<0.05$) from

preceding protein concentration, † Not significantly different from preceding protein concentration.

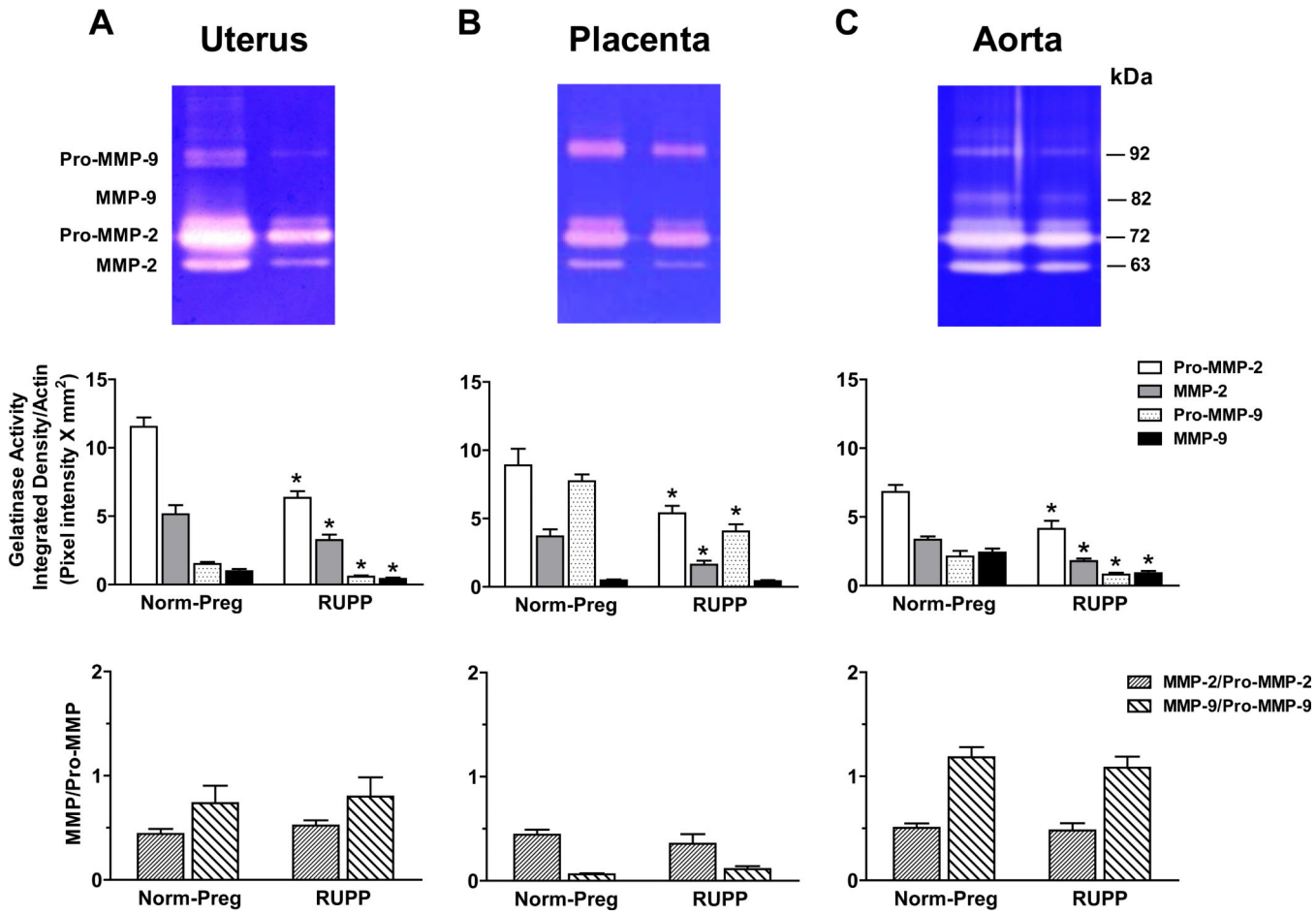

Fig. 4.

Uterine, placental and aortic MMP-2 and MMP-9 gelatinase activity in Norm-Preg and RUPP rats. Equal protein amount (1 μg) of tissue homogenates from the uterus (A), placenta (B) and aorta (C) of Norm-Preg and RUPP rats were prepared for gelatin zymography analysis. The densitometry values of the proteolytic bands corresponding to pro-MMP-2, MMP-2, pro-MMP-9 and MMP-9 was presented as pixel intensity × mm^2 and normalized to β-actin to correct for loading. The MMP-2/pro-MMP-2 and MMP-9/pro-MMP-9 ratios were also measured. Bar graphs represent means±SEM, n = 9/group. * Measurements in RUPP rats are significantly different ($P<0.05$) from corresponding measurements in Norm-Preg rats.

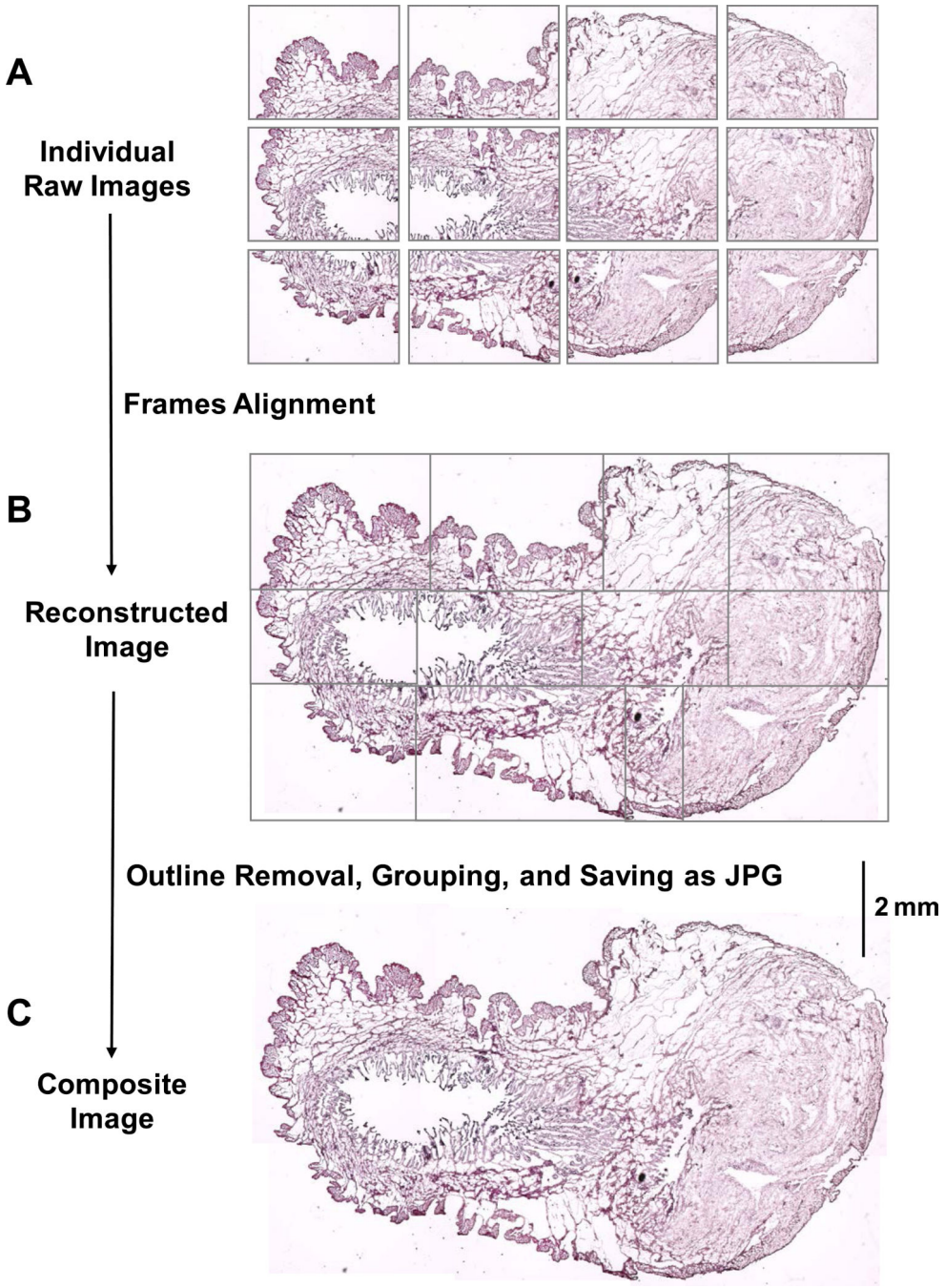

Fig. 5.

Representative reconstructed composite image of Norm-Preg rat uterus tissue section stained with hematoxylin and eosin. Because the rat uterus is large, only a small portion of the tissue section could be imaged using a 4× objective. To circumvent this difficulty, and to perform quantitative histological analysis in the whole tissue section, 15 picture frames of sequential parts of the uterine tissue section were acquired using 4× objective and inserted as individual raw images in Powerpoint (A), the image frames were aligned to produce a reconstructed

image of the uterus (B), then the individual images were grouped and saved as a composite JPG image of the whole reconstituted uterine tissue section for image analysis (C).

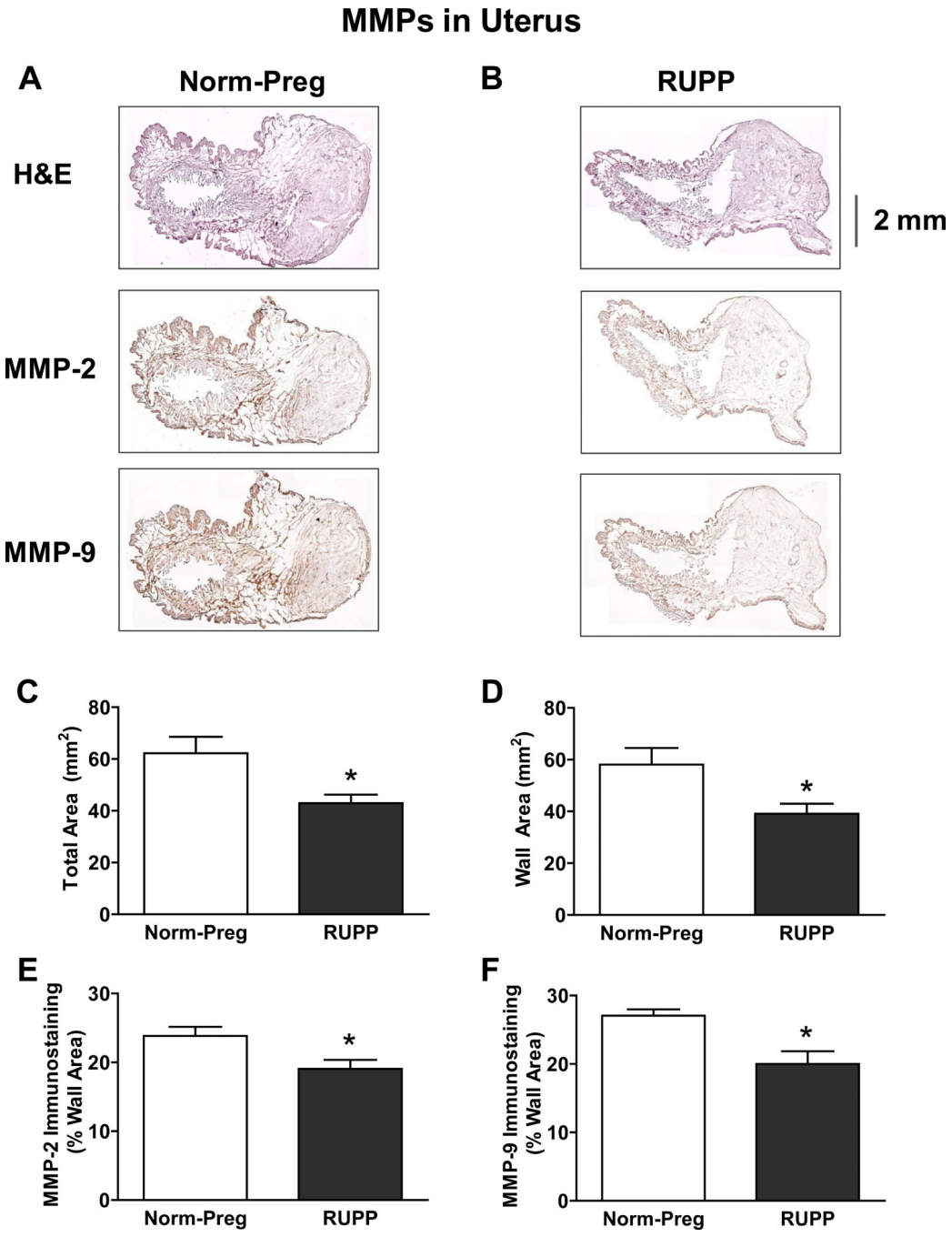

Fig. 6.

Distribution of MMP-2 and MMP-9 in uterus of Norm-Preg and RUPP rats. Cryosections (6 μM) of the uterus of Norm-Preg (A) and RUPP rats (B) were prepared for hematoxylin and eosin staining (H&E), or immunohistochemical staining using MMP-2 and MMP-9 antibodies. Because the rat uterus is large, 10 to 16 picture frames of sequential parts of the uterine tissue section were acquired using 4× objective, and the composite image of the whole uterine section was reconstituted as described in Figure 5, then analyzed using ImageJ software. For the H&E stained tissues, the total number of pixels in the tissue section image

was defined and translated into total area (mm^2) using calibration bar (C), or the wall area (total - lumen) in pixels was measured and presented in mm^2 (D). For MMP immunostaining, the total number of pixels in the tissue section wall was first defined, then the number of brown spots (pixels) was counted and presented as % of total wall area (E and F). Total magnification = 40. Bar graphs represent means±SEM, n = 4 to 6/group. * Measurements in RUPP rats are significantly different ($P<0.05$) from corresponding measurements in Norm-Preg rats.

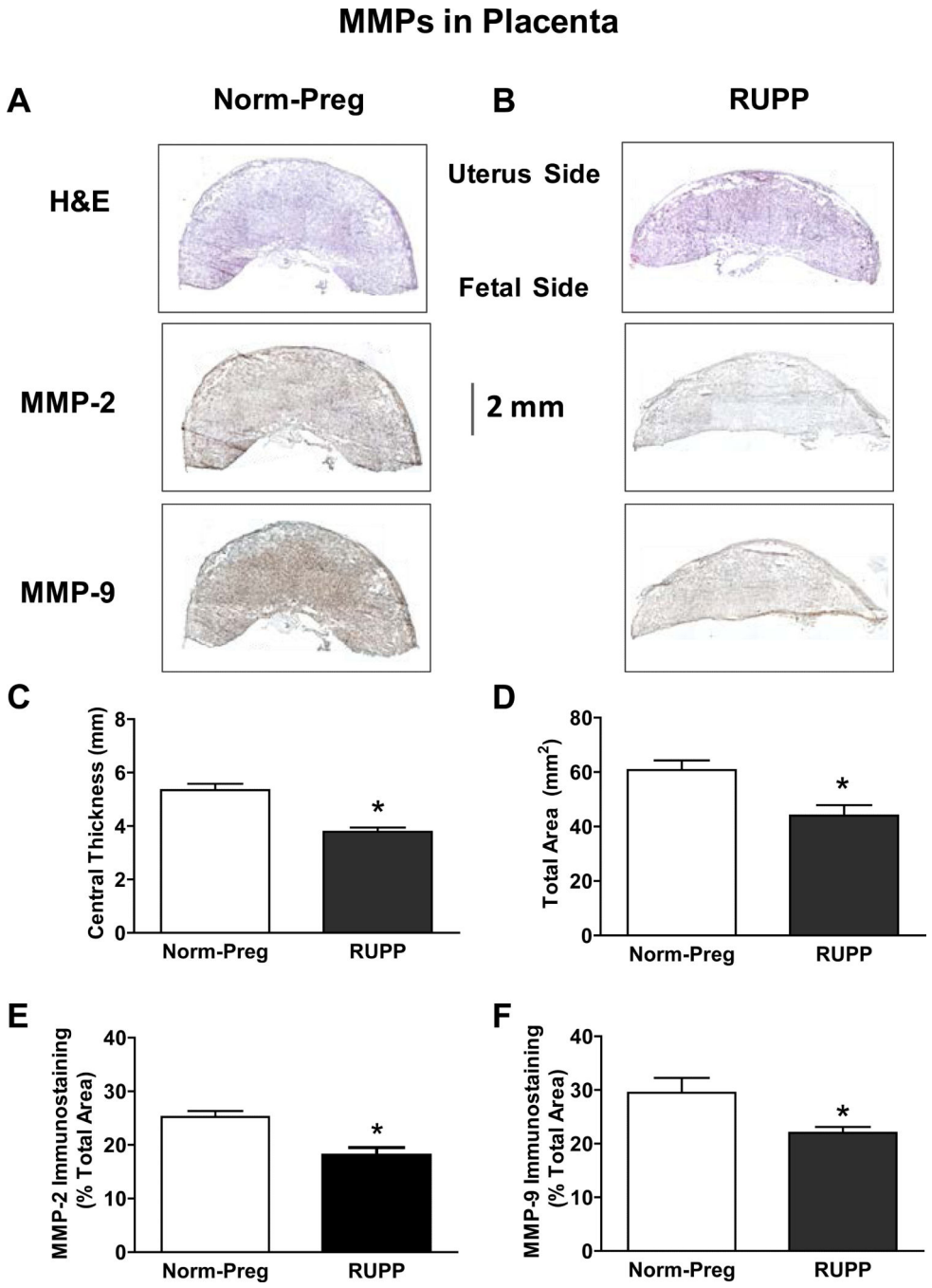

Fig. 7.

Distribution of MMP-2 and MMP-9 in placenta of Norm-Preg and RUPP rats. Cryosections (6 μM) of placenta of Norm-Preg (A) and RUPP rats (B) were prepared for hematoxylin and eosin staining (H&E), or immunohistochemical staining using MMP-2 and MMP-9 antibodies. Because the rat placenta is large, 10 to 16 picture frames of sequential parts of the placental tissue section were acquired using 4× objective, and the composite image of the whole placental tissue section was reconstituted and analyzed using ImageJ software. For the H&E stained tissues, a line scan was drawn in the center of placenta, the number of

pixels in the line were counted and translated into central tissue thickness (mm) using calibration bar (C), or the total number of pixels in the tissue section image was defined and translated into total area (mm^2) using calibration bar (D). For MMP immunostaining, the total number of pixels in the tissue section image was first defined, then the number of brown spots (pixels) was counted and presented as % of total area (E and F). Total magnification = 40. Bar graphs represent means±SEM, n = 4 to 6/group. * Measurements in RUPP rats are significantly different ($P<0.05$) from corresponding measurements in Norm-Preg rats.

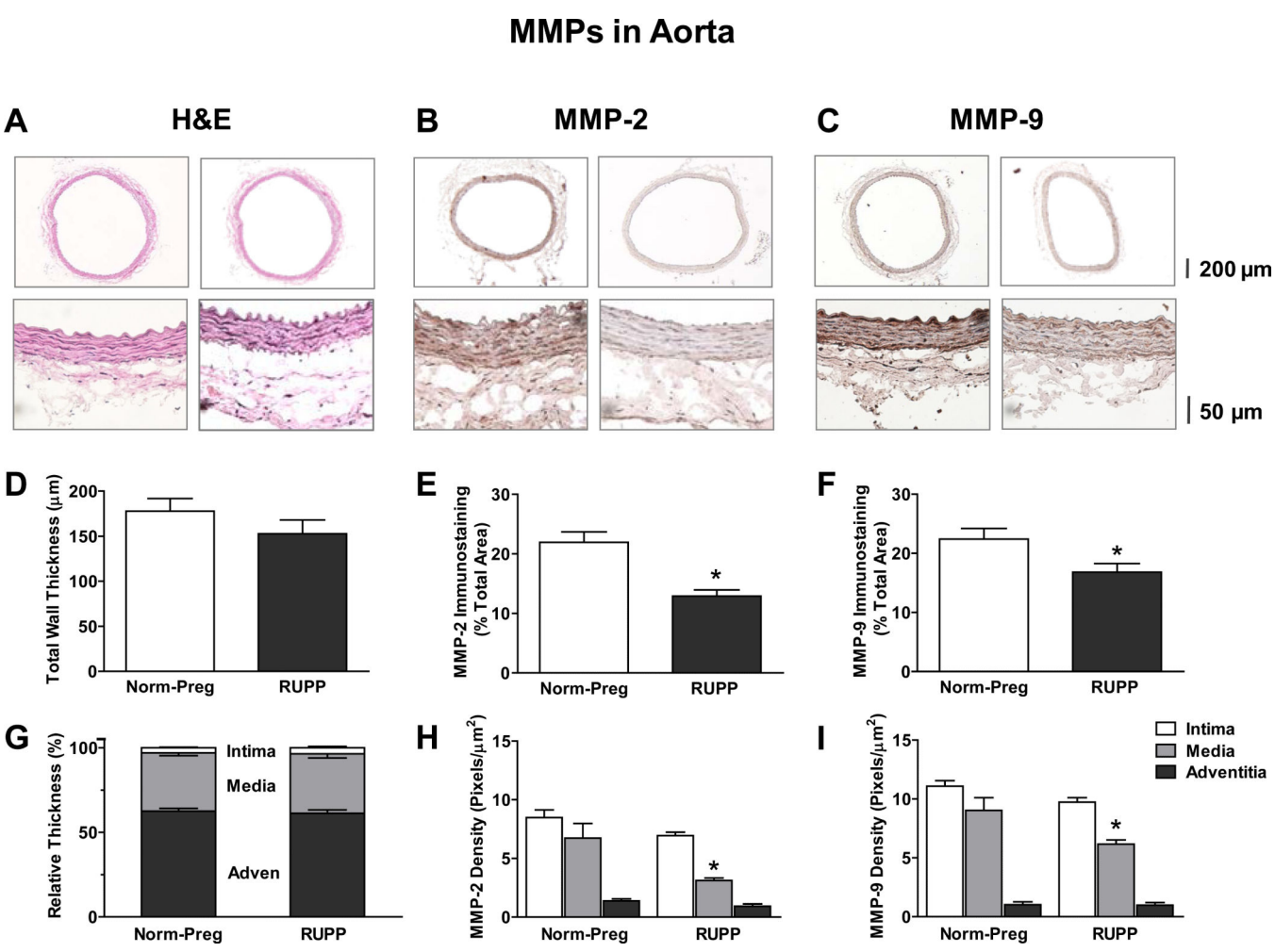

Fig. 8.

Distribution of MMP-2 and MMP-9 in aorta of Norm-Preg and RUPP rats. Cryosections (6 µM) of aorta of Norm-Preg and RUPP rats were prepared for hematoxylin and eosin staining (H&E) (A), or immunohistochemical staining using MMP-2 (B) and MMP-9 antibodies (C). For the H&E stained tissues, a line scan was drawn across the tissue wall, the number of pixels in the line were counted and translated into total wall thickness (µM) using calibration bar (D), or the thickness of the different tissue layers, intima, media and adventitia, was measured and presented as % of total wall thickness (G). For MMP immunostaining, the total number of pixels in the tissue section wall was first defined, then the number of brown spots (pixels) was counted and presented as % of total wall area (E and F). The number of pixels in the specific vascular layer (intima, media and adventitia) was also defined and transformed into the area in μM^2 using a calibration bar. The number of brown spots (pixels) representing MMP-2 and MMP-9 in each vascular layer was then counted and presented as number of pixels/μM^2 (H and I). Bar graphs represent means±SEM, n = 4 to 6/group. * Measurements in RUPP rats are significantly different ($P<0.05$) from corresponding measurements in Norm-Preg rats.

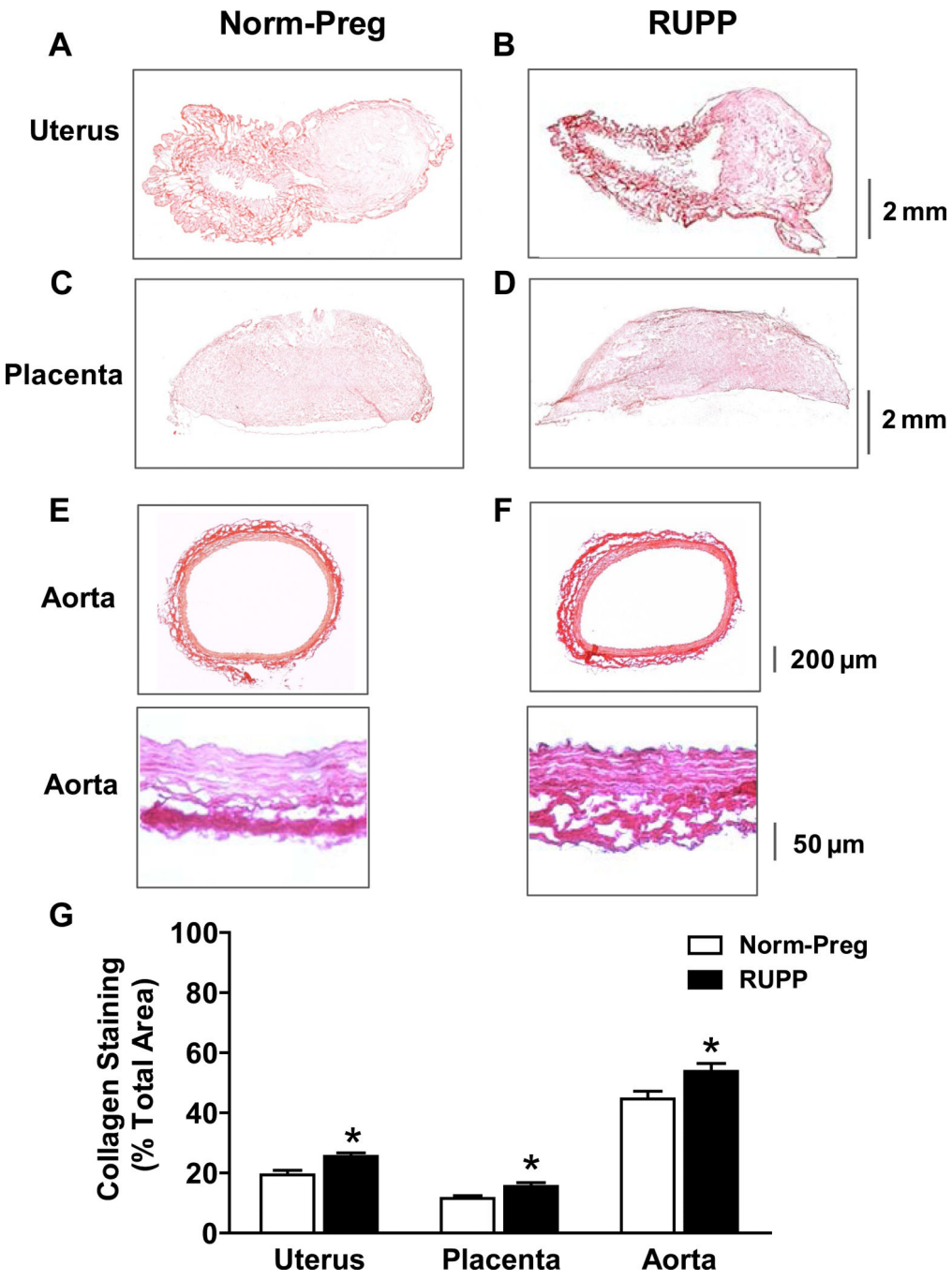

Fig. 9.

Distribution of collagen in uterus, placenta and aorta of Norm-Preg and RUPP rats. Cryosections (6 μM) of uterus (A and B), placenta (C and D) and aorta (E and F) of Norm-Preg and RUPP rats were prepared for Picro-Sirius Red staining for collagen. Because the rat uterus and placenta are large, 10 to 16 picture frames of sequential parts of the tissue section were acquired using 4× objective, and the composite images of the whole uterine and placental tissue section were reconstituted. Representative images of the aorta were acquired using both 10× and 40× objectives. Images of tissue sections were acquired then analyzed

using ImageJ software. The total number of pixels in the tissue section image was first defined, then the number of red spots (pixels) corresponding to collagen was counted and presented as % of total area (G). For uterus and placenta, total magnification = 40. For aorta, total magnification = 100 or 400. Bar graphs represent means±SEM, n = 6/group. * Measurements in RUPP rats are significantly different ($P<0.05$) from corresponding measurements in Norm-Preg rats.

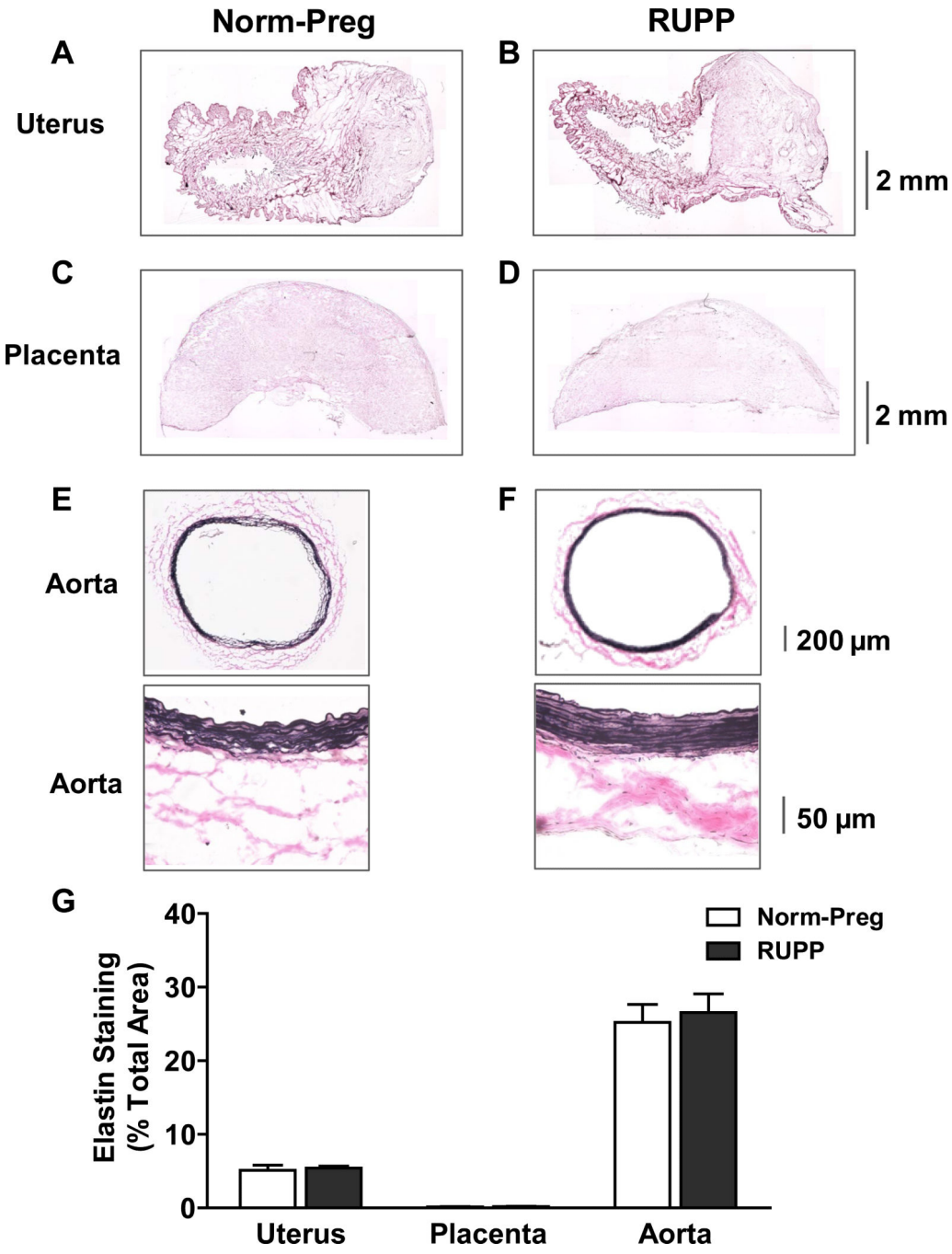

Fig. 10.

Distribution of elastin in uterus, placenta and aorta of Norm-Preg and RUPP rats. Cryosections (6 μM) of uterus (A and B), placenta (C and D) and aorta (E and F) of Norm-Preg and RUPP rats were prepared for Modified Verhoff's-Van Gieson staining for elastin. Because the rat uterus and placenta are large, 10 to 16 picture frames of sequential parts of the tissue section were acquired using 4× objective, and the composite images of the whole cross section of uterus and placenta were reconstituted. Representative images of the aorta were acquired using both 10× and 40× objectives. Images of tissue sections were acquired

then analyzed using ImageJ software. The total number of pixels in the tissue section image was first defined, then the number of black spots (pixels) corresponding to elastin was counted and presented as % of total area (G). For uterus and placenta, total magnification = 40. For aorta, total magnification = 100 or 400. Bar graphs represent means±SEM, n = 6/ group.

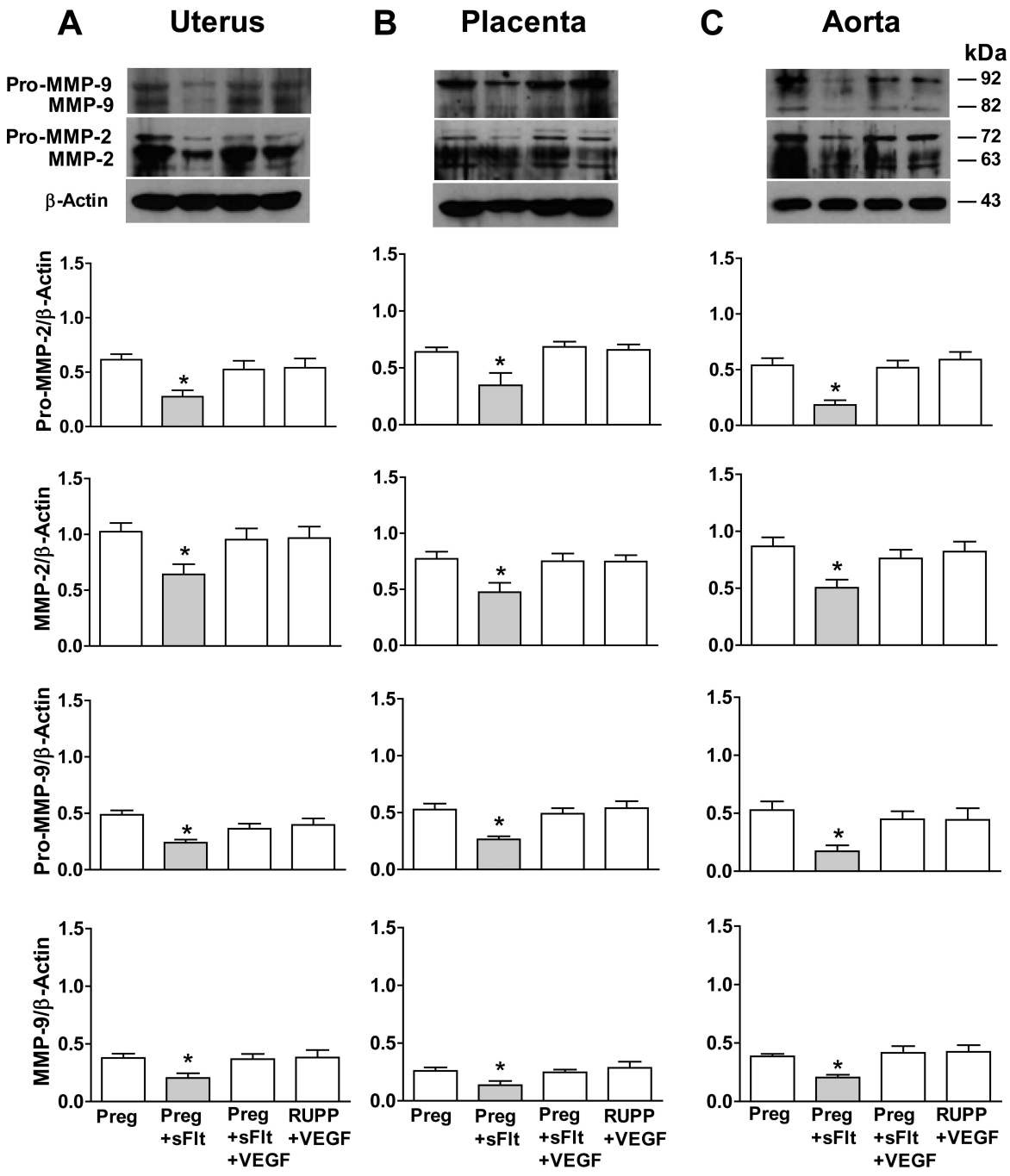

Fig. 11.

Effect of growth modulators sFlt-1 and VEGF on protein amount of uterine, placental and aortic MMP-2 and MMP-9 in Norm-Preg and RUPP rats. Tissue homogenates of the uterus (A), placenta (B), and aorta (C) of Norm-Preg rats were treated with sFlt-1 (0.1 μg/ml) with or without VEGF (0.1 μg/ml), and tissues of RUPP rats were treated with VEGF for 48 hr in organ culture. Tissues were homogenized and prepared for Western blot analysis using antibodies to MMP-2 (1:1000) and MMP-9 (1:1000). Immunoreactive bands corresponding to pro-MMP-2, MMP-2, pro-MMP-9 and MMP-9 were analyzed by optical densitometry

and normalized to β-actin to correct for loading. Bar graphs represent means±SEM, n = 6/group. * Significantly different ($P<0.05$) from corresponding measurements in control non-treated tissues of Norm-Preg rats.

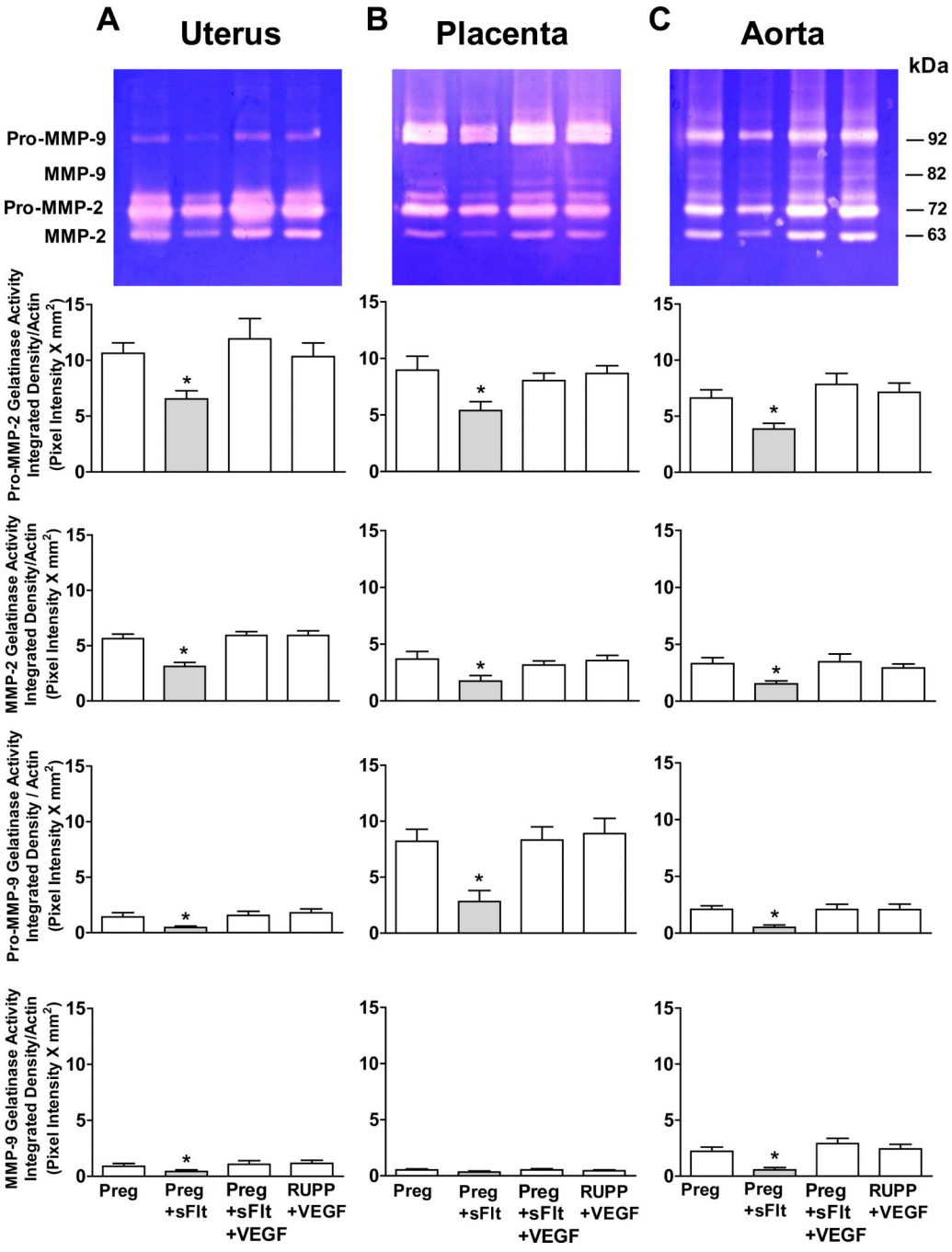

Fig. 12.

Effect of growth modulators sFlt-1 and VEGF on gelatinase activity of uterine, placental and aortic MMP-2 and MMP-9 in Norm-Preg and RUPP rats. Tissue homogenates of the uterus (A), placenta (B), and aorta (C) of Norm-Preg rats were treated with sFlt-1 (0.1 μg/ml) with or without VEGF (0.1 μg/ml), and tissues of RUPP rats were treated with VEGF for 48 hr in organ culture. Tissue homogenates were prepared for gelatin zymography analysis. The densitometry values of the proteolytic bands was presented as pixel intensity × mm^2 and normalized to β-actin to correct for loading. Bar graphs represent means±SEM, n = 6/group.

* Significantly different ($P<0.05$) from corresponding measurements in control non-treated tissues of Norm-Preg rats.